

IDA

INSTITUTE FOR DEFENSE ANALYSES

**Military Applications of Curved
Focal Plane Arrays Developed
by the HARDI Program**

Bohdan Balko
Isaac Chappell
John Franklin
Robert Kraig

January 2011

Approved for public release;
distribution is unlimited.

IDA Document NS D-4268

Log: H 11-000208



The Institute for Defense Analyses is a non-profit corporation that operates three federally funded research and development centers to provide objective analyses of national security issues, particularly those requiring scientific and technical expertise, and conduct related research on other national challenges.

About This Publication

This work was conducted by the Institute for Defense Analyses (IDA) under contract DASW01-04-C-0003, Task DA-2-3256, "Defense Technology Applications and Analyses," for the Defense Advanced Research Projects Agency (DARPA). The views expressed are those of the author and do not reflect the official policy or position of the Department of Defense or the U.S. Government.

Copyright Notice

© 2011 Institute for Defense Analyses
4850 Mark Center Drive, Alexandria, Virginia 22311-1882 • (703) 845-2000.

This material may be reproduced by or for the U.S. Government pursuant to the copyright license under the clause at DFARS 252.227-7013 (NOV 95).

INSTITUTE FOR DEFENSE ANALYSES

IDA Document NS D-4268

**Military Applications of Curved
Focal Plane Arrays Developed
by the HARDI Program**

Bohdan Balko
Isaac Chappell
John Franklin
Robert Kraig

Executive Summary

Digital cameras use a focal plane array (FPA) to convert light energy into electrical energy that can be processed and stored in the memory chip. The FPA is composed of pixels or chips of electro-optical material on a planar surface. Placing the sensors (pixels) on a plane surface can lead to off-axis (spherical) aberrations and can limit the field of view (FOV) of optical systems unless exotic optics are used. To correct for these distortions, designers have to use additional optical elements, which complicate the design of the optics and increase the cost of the cameras.

Curved FPAs with simple spherical lenses would provide improved performance (vs. the commonly used planar FPA). These curved FPAs would provide a large FOV with better resolution off axis, would require fewer lenses, and would eliminate the need for image post processing. The systems that employ these curved FPAs have superior optical properties, but the curved FPAs are more difficult to manufacture. To meet this challenge, the Defense Advanced Research Projects Agency/Microsystems Technology Office (DARPA/MTO) has instituted a program called the Hemispheric Array Detector for Imaging (HARDI). The program's goal is to develop curved FPA technology and combine it with appropriate lens systems to enhance military capability. To accomplish this goal of creating a curved FPA, the HARDI program is exploiting the properties of organic and hybrid organic/inorganic semiconductor materials.

In support of the HARDI program, the Institute for Defense Analyses (IDA) performed technical assessments and provided planning assistance. IDA has identified promising applications of spherical FPAs that could potentially be exploited for defense-related applications. Curved FPAs remove the need for complex lens systems to correct off-axis distortion, and this improvement alone reduces the weight, size, and complexity of lens systems. From the multiple specific applications of curved FPAs identified by IDA (cameras mounted on small robots, miniature unmanned aerial vehicles (UAVs), and small surveillance cameras), HARDI management decided to focus first on the cameras used on small robots for the Advanced Mine Detection System (AMDS) Program. HARDI management then directed IDA to provide an independent analyses of these proposed systems, including appropriate selection of lenses and tradeoff studies of pixel size and count vs. camera characteristics to obtain optimum conditions for various robot camera applications. For this task, IDA developed a ray tracing code, compared this code to published results and simple analytical closed-form solutions, and began using it to study applications of interest to HARDI.

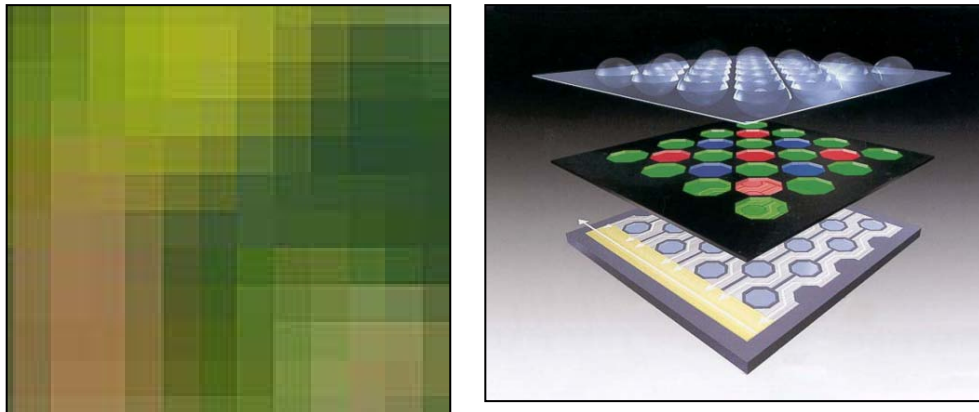
Contents

1.	Introduction	1-1
	A. Background	1-1
	B. HARDI Program/Institute for Defense Analyses (IDA) Task	1-3
	1. HARDI Program.....	1-3
	2. IDA Task	1-4
2.	Potential Military Applications of Curved FPAs	2-1
3.	Cameras Used With Small Robots	3-1
4.	Ray Tracing Code and Analysis	4-1
	A. Ray Tracing Code – Introduction to Terminology.....	4-1
	1. MTF.....	4-1
	2. PSF	4-1
	B. Briefing.....	4-2
	Appendix A. Ray Tracing Codes	A-1
	Illustrations	B-1
	Abbreviations	C-1

1. Introduction

A. Background

Digital cameras use a focal plane array (FPA) to convert light energy into electrical energy that can be processed and stored. The FPA is a two-dimensional (2-D) array of photodetectors (or pixels) fabricated on an electro-optical material. Used in this way, the term pixel refers to the actual physical detector in a camera. In digital imaging, however, a pixel is the smallest addressable picture element in raster graphics—the smallest unit of picture that can be controlled. Figure 1-1 presents both concepts of a pixel. In this report, we will use the concept of pixel represented in Figure 1-1(b).



(a)

(b)

Figure 1-1. Two Usages of the Term Pixel: (a) Pixel Pattern as Used in Imaging and (b) Physical Pixels (Bottom) Forming an FPA, With Micro Lenses (Top) and Color Filters (Center)

The size and the number of the individual pixels affect the resolution and the read-out speed of the camera. The more pixels a digital camera has, the more detail it can record when a photo is taken. Smaller pixels improve resolution, if the camera resolution¹ is not optics limited, but may reduce sensitivity (i.e., need more time for required energy deposition). Modern digital cameras contain FPAs that have pixel counts on the order of megapixels. For example, cameras with 2 megapixels are becoming obsolete, cameras with 5 megapixels are in decline but still a good value, and cameras with 10 megapixels are in the mainstream.

¹ Resolution of systems is generally described by the modulation transfer function (MTF), which is defined and discussed at the beginning of Section 4.

In current digital cameras, a design constraint of optical systems is that the image surface (or Petzval² surface) must be planar so that the image can be recorded on a planar silicon FPA. This requirement leads to off-axis aberrations including spherical, astigmatism, field curvature, and coma. To correct for these distortions, designers use additional optical elements, which complicate the design of the optics and increase the cost of the cameras. Figure 1-2 shows a modern camera with the complex lens system and the flat FPA.

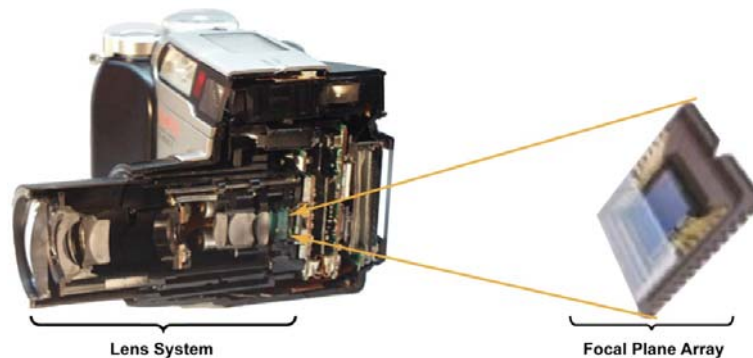


Figure 1-2. Cutout of a Camera Showing the Lens System and the Position of the FPA

To avoid the complexity of lens systems shown in Figure 1-2, the use of curved FPAs with simple spherical lenses has been proposed and is being developed for military applications by the Defense Advanced Research Projects Agency/Microsystems Technology Office (DARPA/MTO) as part of the Hemispheric Array Detector for Imaging (HARDI) program. Figure 1-3 shows ray tracing results for three optical/FPA systems and illustrates the benefits of curved FPAs over the flat-plane FPAs.

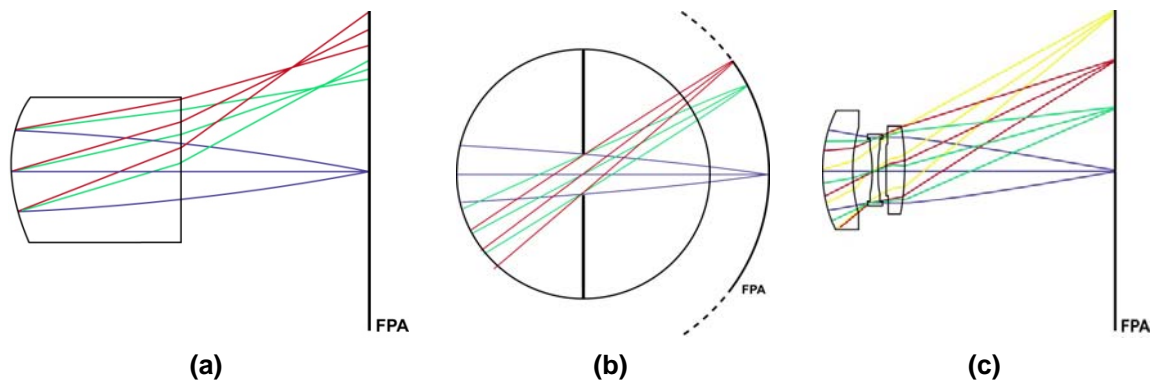


Figure 1-3. Comparison of Ray Tracings for Different Systems

Note for Figure 1-3: (a) Single element lens with a planar FPA, (b) Ball Lens with a curved FPA, and (c) Three-element lens system with a planar FPA.

² Joseph Petzval (1807–1891) was a Hungarian mathematician, inventor, and physicist. He is best known for his work in optics. Petzval is considered one of the main founders of geometrical optics, modern photography, and cinematography. Among his inventions are the Petzval portrait lens and opera glasses, both still in common use today.

Ray tracing results for a single-element plano-convex lens (a commonly used simple lens) on a planar FPA indicate some obvious problems (see Figure 1-3(a)). First, notice that the off-axis rays do not focus on the FPA beyond the center of the FPA. This lack of focus causes blurring of point spots and reduces the resolution of the system. Reduction of relative illumination, referred to as fall-off, at the edge of pictures also occurs because the focal length of the ray does not match the location of the planar FPA. This issue of ray spreading affects proper data collection and will be discussed in more detail in Chapter 4 when we define the point spread functions (PSFs) and modulation transfer functions (MTFs) and use them to compare different lens systems.

The system with the spherical FPA and ball lens with the same center point improves ray focusing and light illumination at different angles. All the rays are axial and pass close to the center of the lens and the FPA sphere because they are constrained by the aperture in the center of the sphere (see Figure 1-3(b)). The symmetry of the system when the rays are constrained to pass through the center of the spherical lens and the spherical FPA allows for a wide field-of-view (FOV).

To maintain good image quality while using a flat FPA, multiple lens systems have to be designed to correct distortions. Figure 1-3(c) illustrates the ray tracing results for a lens system using three lenses and terminating on a flat FPA. Although this shows an improvement over Figure 1-3(a), increasing the FOV can still be a problem.

B. HARDI Program/Institute for Defense Analyses (IDA) Task

1. HARDI Program

State-of-the-art cameras could be improved by increasing their FOVs with uniform illumination over all angles and decreasing their weight and cost. A simple curved FPA would provide this improvement.

Curved FPAs have been suggested as having superior optical properties, but they are more difficult to manufacture and have been restricted to large radii of curvature until recently. New technologies have allowed the manufacture of curved FPAs with diameters as small as 1 cm.

To develop curved FPA technology and combine it with appropriate lens systems to improve military capability, DARPA/MTO has put in place the HARDI program. The objective of this program is to exploit properties of organic and hybrid organic/inorganic semiconductor materials to create a curved FPA. This curved FPA will provide a large FOV that has better resolution off axis, will require fewer lenses, and will eliminate the need for image post processing.

The first two phases of the HARDI program are approaching completion. The intent of the third phase is to provide a useful device for an important military application. In

other words, DARPA needs to focus on a real military problem and optimize the HARDI system to meet the needs of the military. To do this, we need to know the current capabilities of military systems that might be improved.

2. IDA Task

IDA performed technical assessments and provided planning assistance to the HARDI program by evaluating the three different approaches to implementing curved FPAs into military systems. The task statement included these areas for investigation:

- Identify military systems that can be simplified and substantially improved by combining curved FPAs with simple, small lightweight commercial lenses;
- Identify potential innovative applications by combining curved FPAs with simple commercial lenses (e.g., determining the feasibility of using rail-mounted, moving curved FPAs to provide passive three-dimensional (3-D) target imaging: detection, location, and identification); and
- Identify a potential application for using Gradient Index of Refraction (GRIN) lenses with curved FPAs to provide wide FOV optical systems (e.g., gun and weapon sights).

In support of the HARDI program, IDA has initially focused on the first area and has identified promising applications of spherical FPAs that could potentially be exploited for defense-related applications. This discussion is included in Chapter 2 of this report. In the past, flat image planes increased the mass and complexity of camera optics. Curved FPAs—like the eye’s retina—alleviate this problem by removing the need for complex lens systems to correct off-axis distortion. This improvement alone reduces the weight, size, and complexity of lens systems in military applications.

From the multiple specific applications of curved FPAs identified by IDA, HARDI management has decided to focus first on cameras used on small robots and directed IDA to provide information about these cameras (e.g., their technical specifications and operational capabilities). These robots are used in the Advanced Mine Detection System (AMDS) and Explosive Ordnance Disposal (EOD) programs. IDA obtained technical information about some of these cameras and investigated their operational capabilities in the field. This information is provided in Chapter 3 of this report.

IDA was then asked to provide independent analyses of these proposed systems. These analyses included appropriate selection of lenses and tradeoff studies of pixel size and count vs. camera characteristics such as resolution, FOV, and so forth to obtain optimum conditions for various robot camera applications. For this task, IDA developed a ray tracing code (see Appendix A of this document), compared the code to published results and simple analytical closed-form solutions, and began using it to study systems of interest to HARDI. This activity is discussed in Chapter 4 of this report.

2. Potential Military Applications of Curved FPAs

Chapter 2 presents the HARDI Follow-Up Meeting briefing that IDA presented to DARPA/MTO on July 21, 2010.

HARDI Follow-Up Meeting
IDA Support to HARDI
Potential Military Applications
of Curved Focal Plane Arrays (FPAs)

July 21, 2010

Bohdan Balko

IDA

Task Objectives

Evaluate the potential benefits of introducing curved focal plane arrays (FPAs) into military systems:

- Identify systems that can be **simplified and substantially improved** by combining curved FPAs with simple, small lightweight lenses
- Identify **innovative** applications by combining curved FPAs with simple commercial lenses (e.g., feasibility of using rail-mounted, moving curved FPAs to provide passive three dimensional (3-D) target imaging (detection, location, identification))
- Identify potential application for using **Gradient Index of Refraction (GRIN) lenses with curved FPAs** to provide wide field of view (FOV) optical systems (e.g., gun and weapon sights)

Steps To Meet Objectives

- Identification of potential technologies for improvement (Institute for Defense Analyses/Science and Technology Division (IDA/STD) staff)
- Identification of current problems with selected technologies and analyses of potential curved FPA (HARDI*) solutions
- Identification of contacts for discussions: project leaders, contractors, experts
- Meetings, discussions with contacts
- Evaluation of competing approaches

* HARDI = Hemispheric Array Detector for Imaging

Small Robots Used in the Advanced Mine Detection System (AMDS) Program

The small robots have a problem with

- **Tunnel vision.** Like looking through a straw. Reduces information input to the operator and prevents robot from using required information for maneuvering
 - *Current solution.* The developers of the optics and cameras try to alleviate this problem by adding cameras, but this solution adds weight, cost, and complexity
 - *New solution.* Wider field of view (FOV) of curved FPAs would help reduce the lens system complexity, cost, and weight
- **Misidentification of objects.** Results from fuzzy images
 - *Solution.* This problem could be attacked/helped with improved off-axis resolution

Miniature Robot Production Used by AMDs

Contact contractors about the potential for application of curved FPAs

- Robot (PackBot, Warrior)
Contact: Orin Hoffman: ohoffman@irobot.com
- QinetiQ North America (previously known as Foster Miller) (Talon), Peter Wells, Senior Engineer: pwells@foster-miller.com
- Northrop Grumman (Andros HD-I)
(need contact)

Miniature Unmanned Aerial Vehicles (UAVs)

- Miniature UAVs have the same problems as small robots—only more greatly exaggerated because of the lift requirement that limits the size and weight
- The sensor systems and imaging systems need high-resolution and large FOV. Curved FPAs could be used to advantage here
- Contact information:
CENTRA Technology, Inc.
Kevin Pick
Office: 703 894 6543 (ext. 143)
Email: pickk@centratechnology.com
- The Night Vision and Electronic Sensors Directorate (NVESD) Air Systems Division (ASD) collaborates with the Army Research Laboratory (ARL) on imaging systems for UAVs. Need to establish a contact

Other Potential Applications

- Small surveillance camera
 - Mounted in a room or across the street from a door or other place where someone might want to monitor the movement of people, vehicles, and so forth and needs to conduct this surveillance over a wide FOV without edge distortion
 - Contact for this application not identified yet
- Spectral bandwidth opening up new applications
 - No application yet for this FPA based on its broad spectral range
 - Somebody at the Night Vision Laboratory (NVL) should know some good applications here. I have plans to contact NVL

Other Considerations

- **Tools/Analyses**
 - Examine utility of ray tracing codes for comparing the effectiveness of systems
 - Start with known capability and examine potential benefits to be gained with curved FPAs
 - Look for tradeoffs between curved FPAs and GRIN lenses
- **Current Capabilities**
 - For current flat FPAs with wide FOVs, how complex is the lens system? Maximum FOV?
 - Look at the characteristics of current imaging systems (lenses, FPA) used in small robot systems
 - Look at two types of GRIN lenses: with perpendicular and normal variation in index of refraction
 - How big are the GRIN lenses developed at the Defense Advanced Research Projects Agency (DARPA)?
- **Consider Competition**
 - Check to see how wide FOV systems with flat FPAs compare with curved FPA systems
 - Check how well cell phone cameras perform. Compare with the military requirements. These cameras are small and lightweight and have low-cost optics

Summary

- Objectives of task presented
- Steps to meet objectives described
- Systems that would improve by introducing HARDI technology identified
- Some contacts/users identified
- Search for other systems to benefit from HARDI continues

3. Cameras Used With Small Robots

Chapter 3 presents the HARDI Follow-Up Meeting briefing that IDA presented to DARPA/MTO on October 5, 2010.

HARDI Follow-Up Meeting
IDA Support to HARDI
Cameras Used With Small Robots

October 5, 2010

Bohdan Balko
IDA

Task Objectives

Evaluate the potential benefits of introducing curved focal plane arrays (FPAs) into military systems:

- Identify systems that can be **simplified and substantially improved** by combining curved FPAs with simple, small lightweight lenses
- Identify **innovative** applications by combining curved FPAs with simple commercial lenses (e.g., feasibility of using rail-mounted, moving curved FPAs to provide passive three dimensional (3-D) target imaging (detection, location, identification))
- Identify potential application for using **Gradient Index of Refraction (GRIN) lenses with curved FPAs** to provide wide field of view (FOV) optical systems (e.g., gun and weapon sights)

Suggested Military Applications

- Small Robots used in the Advanced Mine Detection System (AMDS) program*
- Miniature unmanned aerial vehicle (UAV)
- Small surveillance camera
- Spectral bandwidth opening up new application

* Erik Rosen/Institute for Defense Analyses (IDA) suggested that we also look into the cameras used by robots in the Explosive Ordnance Disposal (EOD) program, which faces requirements similar to those in the AMDS program

Production of Miniature Robots Used by AMDS

Contacts:

- **iRobot** (*PackBot, Warrior*)
Contact: Orin Hoffman
- **QinetiQ North America** (previously known as Foster Miller)
(*Talon*)
Contact: Peter Wells, Senior Engineer
- **Northrop Grumman** (*Andros HD-1*)
Contact: RemotecService@ngc.com

QinetiQ North America (*Talon*)

Peter Wells, Senior Engineer

Response

- Sent information for two types of cameras used on the *Talon*:
 - PC168-IR (General information)
 - Zoom Camera (Tech Specs sheet)
- Wants to follow the Hemispheric Array Detector for Imaging (HARDI) program progress
- Offered collaboration: “If you reach the point where you want to test a system, let me know and we can set something up”

PC168-IR

- **Randy Williams** (Senior Inside Sales Account Manager) Super Circuits (manufacturer of camera)
- PC168-IR mounted on *Talon* but is a discontinued model
- Replacement: PC177IR-8. It is a 420 TV Line (TVL) camera
- PC168-IR specifications
 - Pixel size: (?)*
 - Effective pixels: 510 x 492
 - Lines of color resolution: 380
 - FOV: 80 deg
 - Size: 4.72 in. diameter, 2.7 in. long



PC168-IR



PC177IR-8

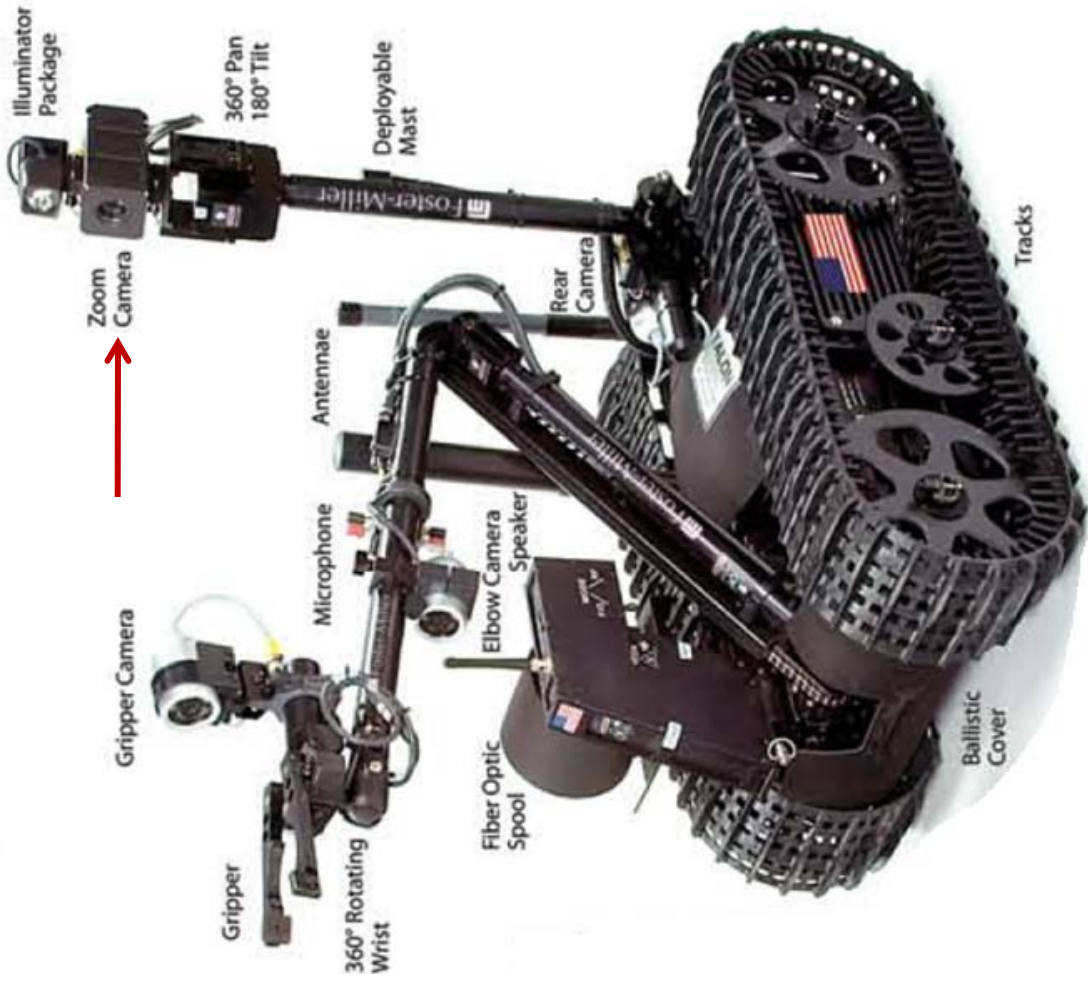
* Pixel size used on another similar camera: 2.85 μm

Zoom Camera on Talon (1)



- Specifications
 - Pixels: 680,000
 - Pixel size: (?)
 - FOV: 42.2 deg
 - Horizontal resolution: 470 TVLs
 - Dimensions: 35.3 x 57.5 x 88.5 mm (W x H x D)
 - Weight: 270 g

Zoom Camera on Talon (2)

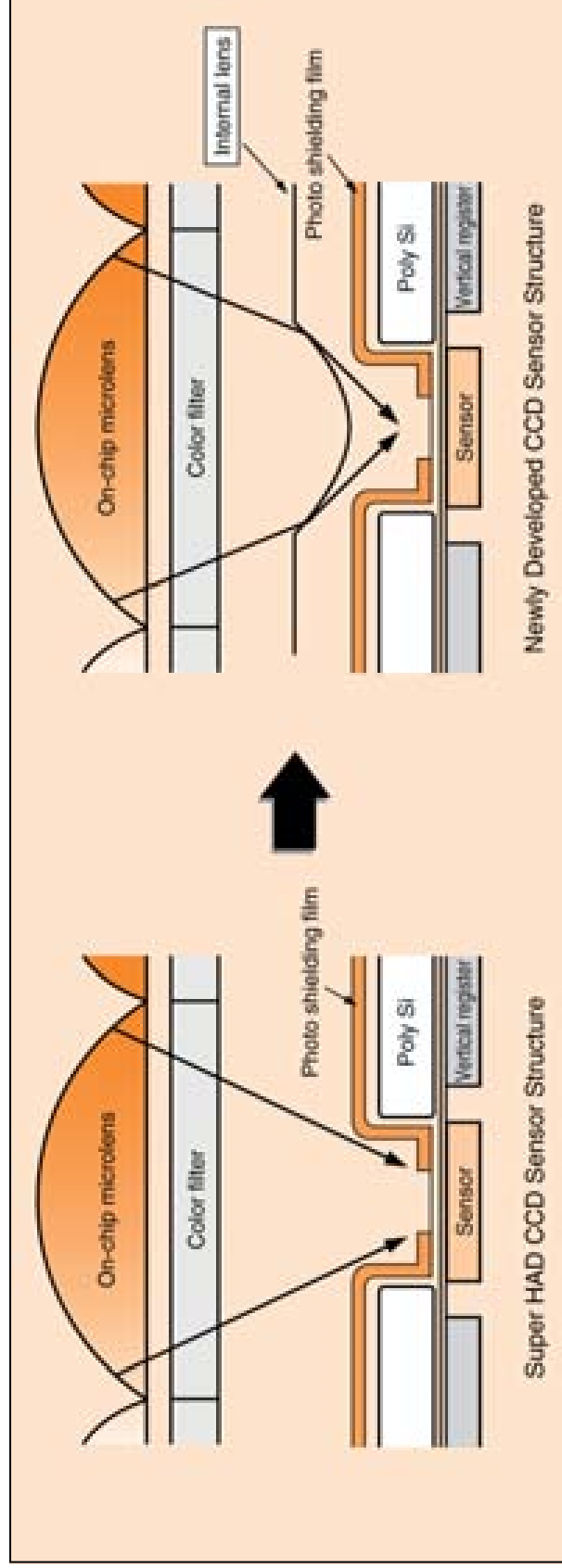


iRobot (*PackBot, Warrior*)

- Christopher Geyer, (Lead Scientist – Imaging Engineer)
- Robots use cameras similar to Sony FCB-EX780B (shown here)
 - Pixel size: $3.2\ \mu\text{m} \times 3.725\ \mu\text{m}$ (micro lenses used)
 - Pixels: 680,000
 - FOV: 45 deg (wide end), 2.0 deg (tele end)
 - Lens: 25X zoom; F 1.6 to F 2.7
 - Signal-to-noise (S/N): 49 dB
 - Dimensions: 50 x 57.5 x 81.8 mm (W x H x D)
 - Weight: 230 g



Micro Lens – Sensor Structure



Other Activity

- I attended QinetiQ robot demonstration at Quantico Marine Base on August 3, 2010. My interest in attending the demo was to see the robots in action and obtain information about the cameras used on the robots
- One robot was equipped with two cameras to produce 3-D imaging. I tried to control the robot's grips with and without 3-D. It was clearly beneficial to have 3-D. I mention this because there may be an innovative way to provide passive, 3-D target imaging with curved FPA cameras

Future Proposed Work

- Conduct a trade study of pixel size and count vs. camera characteristics to obtain optimum conditions for various robot camera applications
- Continue obtaining information about cameras in use on robots in AMDS and EOD programs to get the latest specs
- Compare pixel material developed by HARDI program with material in current cameras. Look at the result if HARDI material was used in a flat FPA for a direct comparison

Backup Slides

- Sony camera
- Sony camera specs
- Zoom camera (QinetiQ)
- Report on micro-lens sensor geometry
- Micro-lens – sensor drawings

Sony FCB-EX780B **25x Super HAD NTSC Color Block Camera with External Syn** *(view product brochure in ADOBE PDF)*



This new FCB-EX780B camera is an evolution in security dome, remote presence and traffic monitoring applications. The FCB-EX780B is equipped with new and unique surveillance features compared to previous FCB models such as an E-flip function that electronically flips the picture for correct image display and an alarm function that enables changes to be detected within any given area of the picture. In addition, this camera features an improved Privacy Zone Masking function compared to previous FCB models for sophisticated masking privacy control - a necessity in many surveillance applications. Combining superb picture quality that you expect from Sony FCB cameras and a variety of unique and convenient features, this new FCB-EX780B camera is the perfect match for demanding indoor and outdoor surveillance applications.

Adding to its superb flexibility and easy operation, the FCB-EX780B camera incorporates familiar and convenient features such as Spot AE, Auto ICR (IR Cut filter removal), quick camera control via a high-speed serial interface (max. 38.4 Kb/s), and various customizable settings.

Features

- E:Flip Function (electronic flip)
- 25x Optical Zoom / 12x Digital Zoom
- Image stabilizer
- Auto ICR (IR Cut Filter Removal)
- Alarm Function
- Day/Night Mode
- Picture Freeze during zoom, focus, preset and lens initializing
- Key switch connector (CN701) and DC/Video Connector (CN903)
- Privacy Zone Masking
- Minimum Illumination of 2.5 lux
- AE Spot
- High-speed serial interface (max. 38.4 kb/s)
- TTL signal-level control (VISCA control)
- Various factory presets
- Internal/External sync
- Lead-free solder, halogen free mounting boards, and low power consumption (min. 1.6W with inactive motors)

Sony Camera Specs

Specifications

Image device	1/6 type Super HAD CCD
Number of Pixels	Approximately 680,000 pixels
Lens	25X zoom, f=2.4 mm (wide) to 60 mm (tele), F1.6 to F2.7
Digital Zoom	12X (300X with optical zoom)
Angle of View	45 degrees (wide end) to 2.0 degrees (tele end)
Min. Object Distance	35 mm (wide end) to 800 mm (tele end)
Sync. System	Internal/External (V-Lock)
Min. Illumination	2.5 lx (typical) (50 IRE)
S/N Ratio	49 dB
Electronic Shutter	1/1 to 1/10,000 s, 22 steps
White Balance	Auto, ATW, Indoor, Outdoor, One-push, Manual
Gain	Auto/Manual (-3 to 28 dB, 2 dB steps)
AE Control	Auto, Manual, Priority mode, Bright, EV compensation, Back-light compensation
EV Compensation	-10.5 to +10.5 dB (1.5 dB steps)
Back Light Compensation	On/Off
Privacy Zone Masking	On/Off (24 positions)
Flicker Cancel	Auto
Focusing System	Auto (Sensitivity: normal, low), One-push AF, Manual, Infinity, Interval AF, Zoom Trigger AF
Picture/Digital Effects	E-Flip, Neg. Art, Black & White, Mirror Image
Camera Operation Switch	Zoom tele, Zoom wide
Video Output:	VBS: 1.0 Vp-p (sync negative), Y/C Output
Camera Control Interface	VISCA (TTL signal level), baud rate: 9.6 Kb/s, 19.2 Kb/s, 38.4 Kb/s, Stop bit: 1/2 selectable
Storage Temp	-20°C to 60°C (-4°F to 140°F)
Operating Temp	0°C to 50°C (32°F to 122°F)
Power Consumption	6 V to 12 V DC, 1.6 W (motors inactive)/2.5 W (motors active)
Weight: approx.	230 g (8.1 oz)
Dimensions	50 x 57.5 x 81.8 mm (2 x 2-3/8 x 3-1/4 inches)

Zoom Camera (QinetiQ)



SPECIFICATIONS:

Image device: 1/4-type Super HAD
Effective pixels: Approx. 680,000 pixels
Digital zoom: 12X (312X with optical zoom)
Horizontal viewing angle: 42.2° (wide end) to 1.6° (tele end)
Minimum object distance: 320 mm (wide end), 1500 mm (tele end)
Sync. system: Internal/External (V-LOCK)
Electronic shutter: 1/1 s to 1/10,000 s, 22 steps
White Balance (WB): Auto / ATW / Indoor / Outdoor / One-Push / Manual
Gain: Auto / Manual (-3 to 28 dB / 2 dB steps)
EV compensation: -10.5 to +10.5 dB (1.5 dB steps)
Backlight compensation: On/Off
Privacy Zone Masking: ON/OFF (24 position)
Flicker cancel: Auto
Focusing system: Auto (sensitivity: Normal and Low), One-Push AF / Manual / Infinity / Interval AF / Zoom Trigger AF
Camera operation / zoom switch: Zoom tele / Zoom wide
Picture effect: E-flip / NEGA Art / Black & White / Mirror Image
Exposure control: Auto / Manual / Priority mode / Bright / EV compensation / Backlight compensation
Lens value: 26X
S/N ratio: More than 50 dB
Minimum illumination: 1.0 lux
Video output: VBS: 1.0 Vp-p (Sync. Negative) / Y/C Output
Signal System: NTSC
Horizontal resolution value: 470 TV lines
Camera control interface: VISCA (TTL signal level) Baud Rate: 9.6 Kb/s / 19.2 Kb/s / 38.4 Kb/s / 1 or 2 Stop bit selectable
Dimensions: (W x H x D), 2 1/4 x 2 3/8 x 3 1/2 inches (55.3 x 57.5 x 88.5 mm)
Weight: 8.1 oz (230g)
Operating temperature: 32 °F to 122 °F (0 °C to 50 °C)
Storage temperature: -4 °F to 140 °F (-20 °C to 60 °C)
Power consumption: 1.6 W (motors inactive) / 3.3 W (motors active)
Power requirements: 6 to 12 VDC

1/6-inch 380K/440K Effective Pixel
Ultrasmall High-picture Quality Camera CCDs

ICX238AKE (NTSC) ICX239AKE (PAL)

There are now increasingly strong demands for even further miniaturization and improved picture quality in CCD devices, which are widely used for image input.

Sony has now developed two new high picture quality ultrasmall CCD image sensors to respond to these demands.

By developing the industry's smallest unit pixel, a pixel with a horizontal pixel pitch of only 3.2 μm , Sony has achieved effective pixel counts of 380K and 440K in the ICX238AKE and ICX239AKE, which are 1/6-inch optical system devices, and Sony has also achieved even further reductions in device power consumption in these products.

These features can contribute to increased picture quality, further miniaturization, and reduced power consumption in digital cameras.

The ICX238AKE (NTSC) and ICX239AKE (PAL) are 1/6-inch optical system color CCD image sensors with 380K and 440K effective pixels, respectively. Despite being ultrasmall devices, they provide the high level characteristics required by camcorders, surveillance cameras, and similar products. Furthermore, since they achieve the low power consumption and other characteristics required by notebook personal computers, PDAs, and other portable information terminals, they are optimal for use in a wide range of applications.

V O I C E

Despite being ultrasmall devices, these CCDs achieve excellent picture quality and high performance. Thus we think that these are optimal CCDs not only for current products that use CCDs, but for products in new application areas that desire image input functionality. I recommend that you will look into using the ICX238AKE or ICX239AKE in unique new products that can take advantage of the miniature size and low power consumption that are the features of these devices.

Further Miniaturization and Higher Picture Quality

Due to the development of fine fabrication technology that can create devices with a horizontal pixel pitch of 3.2 μm , which corresponds to the industry's smallest unit pixel, Sony achieved effective pixel counts of 380K and 440K, which are the largest pixels for a 1/6-inch optical system device. Thus these devices achieve both further miniaturization and higher picture quality. (See figure 1.)

Improved Basic Characteristics

A newly developed optical structure was introduced in these devices. This structure adds internal lenses above the photo shielding film to the Sony Super HAD CCD technology. (See figure 2.) By further optimizing the lens shape using an optical simulator, Sony was able to increase the sensitivity per unit area by 48% over Sony 1/4-inch CCDs with the same number of pixels, thus achieving a level of 300 mV.

The saturation signal level was also improved by 65% on a per unit area basis by optimizing the sensor structure, achieving values of 600 mV (NTSC) and 540 mV (PAL). Thus these devices achieve excellent performance in their imaging characteristics despite being miniature devices. (See table 2.)

- **Further miniaturization and higher picture quality**
Due to the development of the industry's smallest unit pixel, these devices achieve the largest number of pixels in a 1/6-inch optical system device.
- **Improved basic characteristics**
The sensitivity per unit area has been increased by 48%, and the saturation signal level has been increased by 65%.*
- **Power consumption reduced by 38%***

*: As compared to Sony 1/4-inch devices with the same number of pixels.

Reduced Power Consumption

Current consumption was reduced by optimizing the output circuits, and furthermore, power consumption was reduced by 38% over Sony 1/4-inch CCDs with the same number of pixels by reducing the capacitance of the transfer register. These devices achieve the lower power consumption of 88 mW, including the driver power consumption. (See figure 3.)

Device Specifications

The specifications of these devices, including the number of pixels and the drive specifications, are identical to those of current Sony 1/4-inch CCDs with the same number of pixels. This means that current system IC products can be used without modification. (See table 1.)

Micro Lens – Sensor Drawings

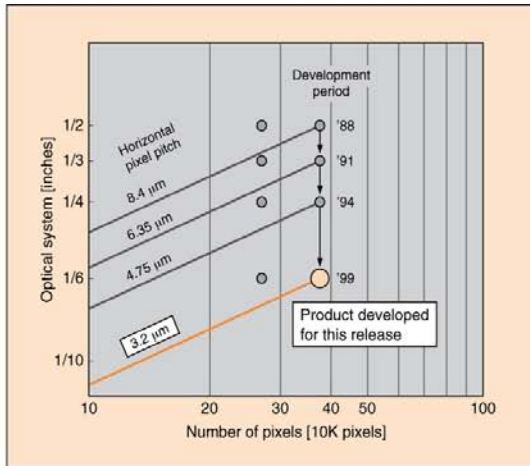


Figure 1 Trends in CCD Development

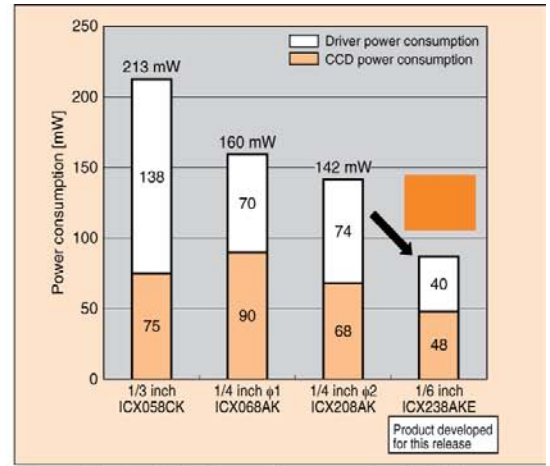


Figure 3 Trends in Power Consumption in 380K-pixel CCDs

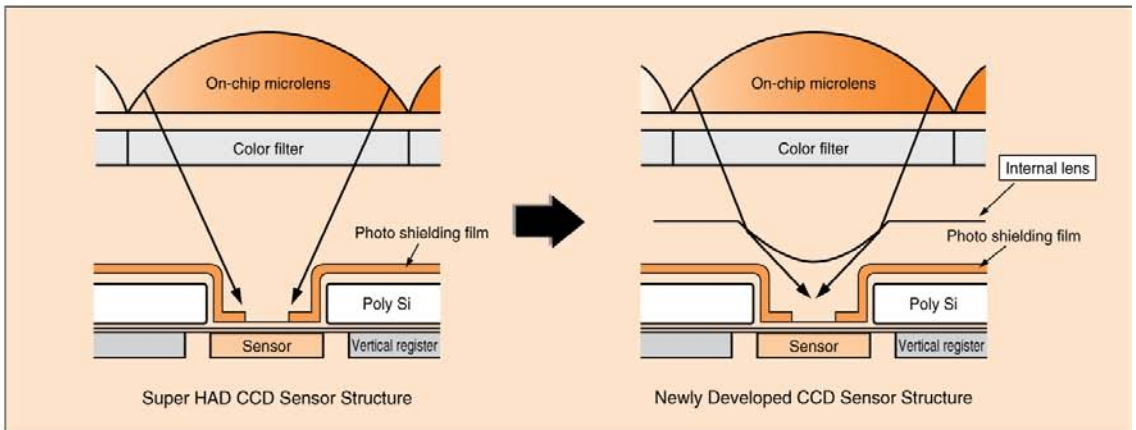


Figure 2 Sensor Structure Comparison

Table 1 Device Structure

Item	ICX238AKE	ICX239AKE
Optical size	1/6-inch format	1/6-inch format
TV format	NTSC	PAL
Transfer method	Interline transfer	Interline transfer
Total number of pixels	811H x 508V Approximately 410K pixels	795H x 596V Approximately 470K pixels
Number of effective pixels	768H x 494V Approximately 380K pixels	752H x 582V Approximately 440K pixels
Chip size	3.30 mm (H) x 2.95 mm (V)	3.30 mm (H) x 2.95 mm (V)
Unit cell size	3.200 μm (H) x 3.725 μm (V)	3.275 μm (H) x 3.150 μm (V)
Horizontal drive frequency	14.3182 MHz	14.1875 MHz
Package	12 pin SON (Ceramic) 9.25 mm (H) x 8.00 mm (V) x 2.30 mm (t)	12 pin SON (Ceramic) 9.25 mm (H) x 8.00 mm (V) x 2.30 mm (t)

Table 2 Imaging Characteristics

Item	ICX238AKE	ICX239AKE	Remarks
Sensitivity F5.6	300 mV	300 mV	3200K, 706 cd/m ²
Saturation signal level	600 mV	540 mV	Ta = 60°C
Smear F5.6	-86 dB	-86 dB	V/10 method

4. Ray Tracing Code and Analysis

A. Ray Tracing Code – Introduction to Terminology

IDA developed a ray tracing code (see Appendix A of this document) that was used to analyze optical systems. With this code, we calculated the MTF and PSF to get a quantitative comparison of the resolution of different optical systems. The resolution is determined by comparing the object test pattern with the resulting image pattern at different spatial frequencies (see Figure 4-1).

1. MTF

The MTF describes the loss of detail in the imaging process as the convolution of the object function (i.e., the ideal image function) with the impulse response of the imaging system. A convolution is an integral that expresses the amount of overlap of one function, h , as it is shifted over another function, f . It “blends” one function with another. The convolution in the spatial domain is a multiplication in the frequency domain. Thus, if $f(x,y)$ is the object function and $h(x,y)$ is the impulse response of the imager, then

$$\mathcal{F} g(x,y) = \mathcal{F} [f(x,y) \times h(x,y)], \quad (4-1)$$

where \mathcal{F} stands for Fourier transform and leads to

$$G(\xi,\eta) = F(\xi,\eta) \times H(\xi,\eta), \quad (4-2)$$

where x, y are the spatial coordinates and ξ, η are the spatial frequency components such that if X, Y are the spatial periods of the object pattern, then $\xi = 1/X$ and $\eta = 1/Y$. F denotes the object spectrum, $H(\xi,\eta)$ is the optical transfer function, and MTF is defined as $|H(\xi,\eta)|$.

We compared the MTF of optical systems obtained with our code and the published results obtained by other investigators. In addition to this comparison, we also compared our code’s results with analytical solutions for simple systems, where we derive an analytical form for an MTF of a sine function with a Gaussian PSF and calculate the MTF with a mathematical program following the analytical closed-form derivation. This comparison is also discussed Appendix A.

2. PSF

The PSF describes the fuzzy image of a point projected by the optical system and is represented by $h(x,y)$ for real systems. For ideal systems the response of the imager is identical to the object function, so $h(x,y) = \delta(x,y)$ or the delta function. The PSF is related

to the MTF. By taking the Fourier transform in two dimensions of the PSF and then taking the absolute value of the result, we obtain the MTF.

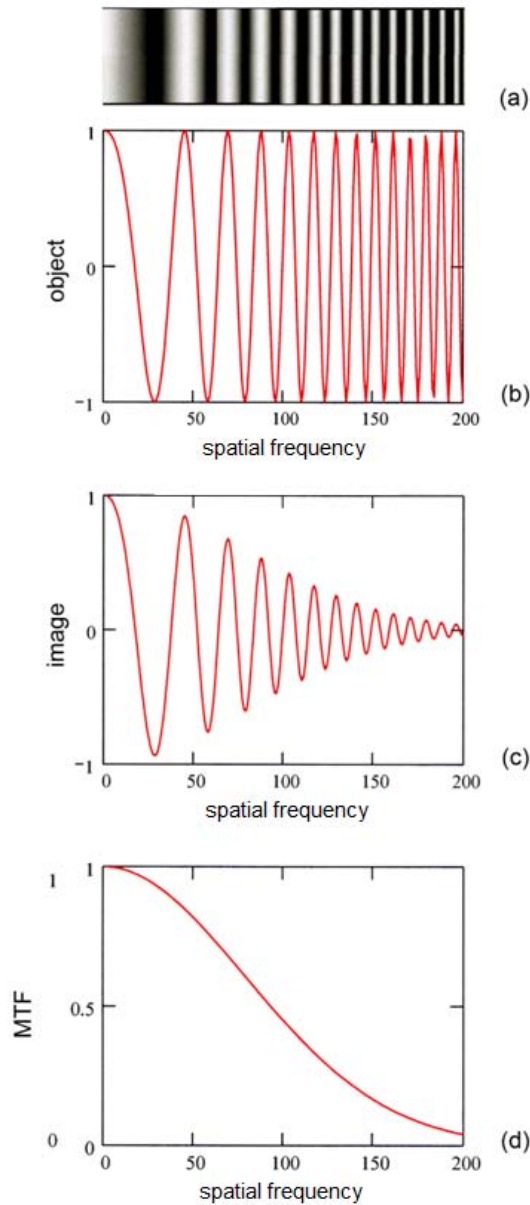


Figure 4-1. The Spatial Frequency of an Object Pattern With the Resulting Image Pattern at Different Spatial Frequencies

Note for Figure 4-1: This figure shows spatial frequency variation in object to MTF of optical system. It shows (a) the object with varying special frequencies, (b) the variation of intensity as a function of special frequency, (c) the image variation of intensity as a result of an imperfect optical system, and (d) the calculated MTF of the system.

B. Briefing

The remainder of Chapter 4 presents the HARDI Follow-Up Meeting (annotated) briefing that IDA presented to DARPA/MTO on January 4, 2011.

HARDI Follow-Up Meeting IDA Support to HARDI

Ray Tracing Analysis

January 4, 2011

Bohdan Balko
IDA

3

For this meeting, I summarized the task work completed before October 5, 2010, and then described a ray tracing code that we developed and verified to help us conduct tradeoff studies.

Task Objectives

Evaluate potential benefits of introducing curved focal plane arrays (FPAs) into *military* systems

- **Simplified and substantially improved** with curved FPAs
- **Innovative** applications (e.g., passive three-dimensional (3-D) imaging)
- **Gradient Index of Refraction (GRIN) lenses with curved FPAs**

4

The question is, how can we improve military systems by reducing the size, weight, complexity, and, therefore, the cost of existing systems? What are some innovative ways to solve problems previously not possible with plane focal plane arrays (FPAs)? How can we combine Gradient Index of Refraction (GRIN) lenses with curved FPAs in an optimized way?

Suggested Military Applications

- Small robots used in the Advanced Mine Detection System (AMDS) program
- Robots used in the Explosive Ordnance Disposal (EOD) program
- Miniature unmanned aerial vehicle (UAV)
- Small surveillance camera
- Spectral bandwidth opening up new applications

5

We found military applications and presented them at the first Hemispheric Array Detector for Imaging (HARDI) follow-up meeting that I attended in July 2010. The sponsor selected small robots used in mine detection and instructed IDA to learn about the characteristics of the cameras used on the robots. Specifically, the HARDI team wanted to know the pixel size or pitch, the number of pixels in the FPA, and the field of view (FOV), along with other parameters (e.g., dimensions).

Robots and Their Cameras

- **iRobot** (*PackBot, Warrior*)
Contact: Orin Hoffman
- **QinetiQ North America** (formerly Foster Miller) (*Talon*)
Contact: Peter Wells, Senior Engineer

6

The robot manufacturers and their representatives listed in this slide provided the information.

Cameras Used on Robots

PC168-IR on *Talon*
FOV: 80 deg
Pixel size: 2.85 μm



Zoom Camera on *Talon*
Pixels: 680,000
FOV: 42.2 deg



iRobot (*PackBot*, *Warrior*)
Sony FCB-EX780B
Pixel size: 3.2 μm x 3.725 μm
Pixels: 680,000
FOV: 45 deg (wide end), 2.0 deg (tele end)



7

The three cameras about which I was able to obtain information are shown in this slide. More detailed specification sheets were appended to the original briefing presented to the HARDI group in October 2010 (see Chapter 3 of this document).

Other Activity

- I attended QinetiQ robot demonstration at Quantico Marine Base on August 3, 2010. My interest in attending the demo was to see the robots in action and obtain information about the cameras used on the robots
- One robot was equipped with two cameras to produce 3-D imaging. I tried to control the robot's grips with and without 3-D. It was clearly beneficial to have 3-D. I mention this because there may be an innovative way to provide passive, 3-D target imaging with curved FPA and *one camera*

Future Proposed Work (10/5/2010)

- Conduct a trade study of pixel size and count vs. camera characteristics to obtain optimum conditions for various robot camera applications
 - To prepare for this trade study, we developed a ray tracing code and investigated a well-known recent publication on curved detectors
- Continue to obtain information about cameras used on robots in AMDS and EOD programs to get the latest specs
- Compare pixel material developed by the Hemispheric Array Detector for Imaging (HARDI) program with material in current cameras. Look at the result if HARDI material was used in a flat FPA for a direct comparison

9

At the October 5th HARDI follow-up meeting, I proposed to conduct a tradeoff study to determine the optimum parameters for the HARDI systems to be designed for various applications.

To do this, we needed a tool—computer code—to study the effects of various parameters that affect the system design.

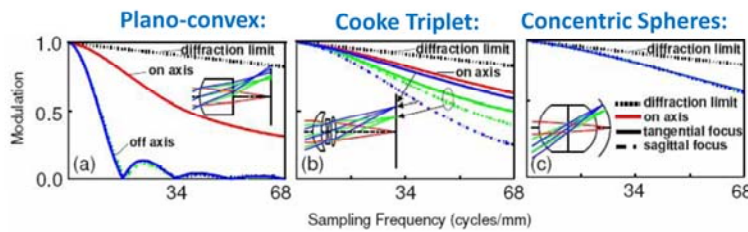
We studied the characteristics of spherical FPA published by the Stanford Group and intended to compare the results of the IDA code using the same parameters and geometry.

Analysis of Stanford Paper on Curved FPAs

Rim, S-B., B. Catrysse, R. Dinyari, K. Huang, and P. Peumans. 2008. "The Optical Advantages of Curved Focal Plane Arrays." *Optics Express* 16 (7): 4965–4971.

Stanford Publication

- The authors investigate the potential advantages to optical imagers of replacing the standard planar imaging surface with a hemispherical detector
- The authors assert that with spherical symmetry (with concentric optics and detector), any object point can be considered “on-axis”
 - This would remove the distinction between tangential and sagittal rays
 - It would also eliminate four out of five Seidel aberrations (coma, astigmatism, field curvature, and distortion)
- System is ostensibly designed for wide field-of-view (FOV) applications
 - Symmetry becomes more advantageous as FOV increases
 - With the small focal lengths being considered here (~6 mm), angular resolution will never approach the capabilities of a modern narrow FOV imager
- Authors have modeled the proposed system and compared it to two other systems. At $f/3.5$, the proposed system seems to outperform the others:



11

The figures at the bottom of this slide give the MTFs calculated by the Stanford group for three different lens systems. The view on the right shows the MTF for the ball lens. An interesting observation is a comparison between the diagram for the ball lens and the two more traditional systems. The left and middle figures appear to present rays that can pass anywhere through the lens systems. However, in the figure on the right, all the displayed rays traverse the lens fairly close to its center, as if an aperture were located in the center of the ball. The paper does not mention an aperture in the center of the nor does it discuss the different constraints imposed on the systems.

Code Development at IDA

- To study the effects of the various system parameters and investigate the tradeoffs, we developed a ray tracing code for calculating the modulation transfer function (MTF) of systems-of-interest, along with their characteristics (MATLAB)
- We checked the code by comparing it with published results (i.e., Rim, S-B., et al., “The Optical Advantages of Curved Focal Plane Arrays”)
- Two system geometries used with different aperture positions
- We also obtained an analytical (closed-form) MTF result for a simple system and studied the result for various spatial frequencies and point spread functions (PSFs) using Mathematica and Mathcad
- Satisfied that the MATLAB code gives reasonable results, we are ready to conduct tradeoff studies

12

This slide describes the IDA code development and verification procedures.

IDA Ray Tracing Model Characteristics

Characteristics of base model:

- Diffraction is ignored
- The lens is a sphere, characterized by a single real index of refraction
- Computations are performed in one plane (meridional)
- Meridional PSFs and MTFs are calculated

We can include diffraction, dispersion, skew rays, multi-dimensional PSFs and MTFs, and more general optical materials (GRIN lenses) and configurations in subsequent versions. We can also modify the FPA surface to study more general shapes (i.e., parabolic FPAs)

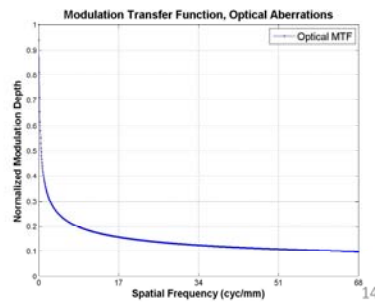
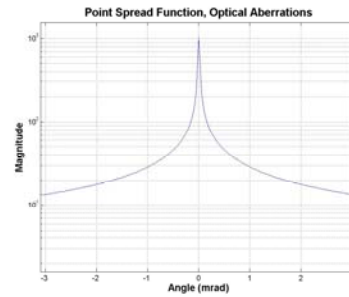
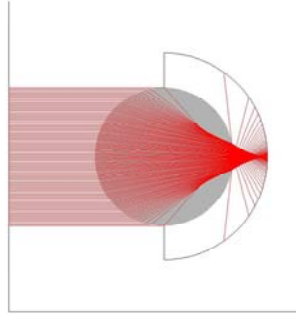
13

This slide describes technical characteristics and assumptions of the IDA model.

Simple Example of Results Form IDA Model

Aperture width = 180 deg
Object Angle = on axis
Object distance \gg Lens radius
Index of refraction: $n_{\text{LENS}} = 1.5$
Lens radius: $r_{\text{LENS}} = 4.0$ mm
Detector radius: $r_{\text{DETECTOR}} = 6.0$ mm
(i.e., detector is at focal position)

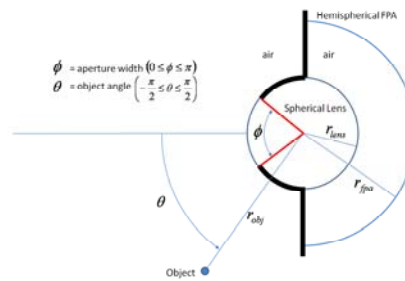
Diagram of Optical System and Detector



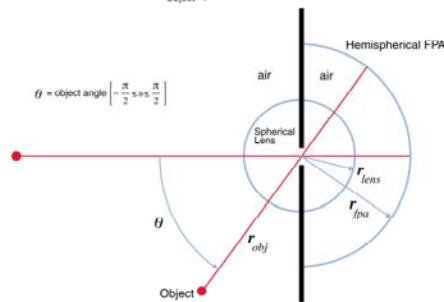
This example shows some of the output that we can produce with our code. The upper left box shows the parameters used in the calculation. First, we produce the ray traces shown in lower left diagram. Although we use many more rays than shown, we only display these few selected ones to prevent confusion. The upper right diagram is the PSF, and the lower right diagram is the aberration MTF (blue line) and the detector pixel MTF (blue line).

Depiction of Aperture Geometries Tested

Geometry I



Geometry II

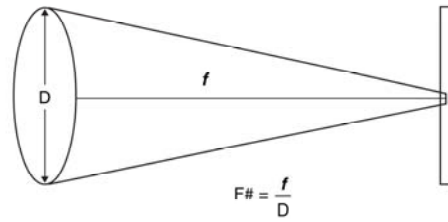


15

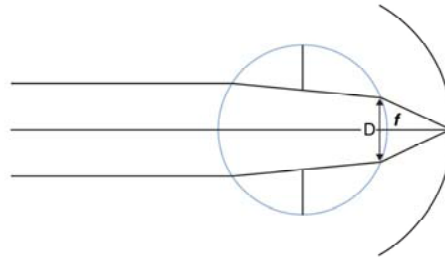
This slide shows two different geometries used in our calculations. The difference between these geometries is the position of the aperture. Geometry I uses an aperture at the ray entry to the lens. Geometry II places the aperture in the plane crossing the center of the ball lens. In Geometry II, all the rays are effectively close to axial. For Geometry I calculations, we used an $f\#$ given by focal length divided by aperture diameter. For Geometry II, we have redefined $f\#$ based on the slope of the exit cone only.

Defining F# for Thick and Thin Lenses

Thin Lens



Appropriate Definition
for Ball Lens



16

This slide shows the geometric parameters traditionally used to calculate F# for a thin lens system (above) and what we feel is appropriate for the ball lens (below).

This is a crucial criterion to match appropriately because the spatial extent of aberration PSF is proportional to $\frac{1}{(F\#)^3}$ (in the small-angle limit).

IDA Calculation: Geometry I

- For the conditions specified in the Stanford paper, the IDA model for Geometry I gives reasonable results, although somewhat less sanguine than those presented earlier:

F# = 3.5: Identical to Stanford

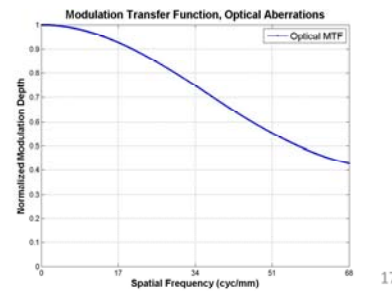
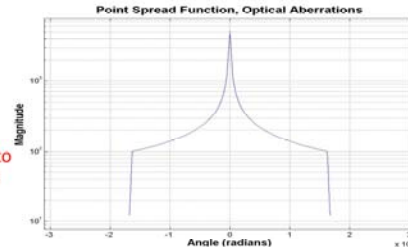
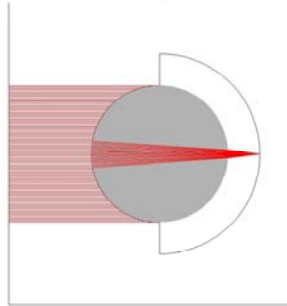
Lens radius = 4 mm: Identical to Stanford

$n_{\text{LENS}} = 1.5168$ (n_d for BK-7 glass): Stanford used a weighted sum of the response at Fraunhofer lines C (H), F (H), and d (He)

$n_c = 1.51432$, $n_f = 1.52238$, $n_d = 1.51680$

Detector radius (and position) = 5.87 mm: Identical to Stanford. Note that this is the focal length of the lens (at n_d)

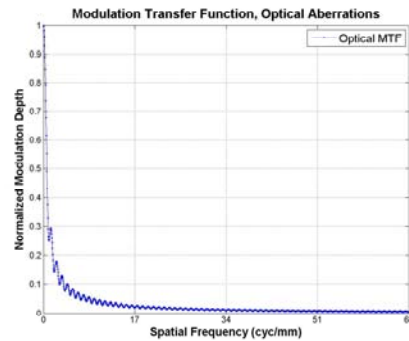
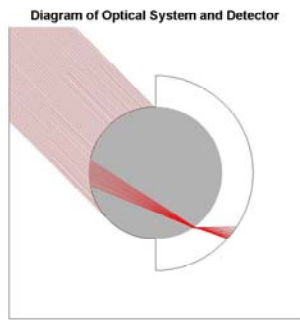
Diagram of Optical System and Detector



The Stanford paper shows an MTF of about 0.6 (~0.75 of the diffraction limit) at 68 cyc/mm. Our computation yielded an MTF of 0.42 at 68 cyc/mm.

Geometry I: Off-Axis Behavior

- We have only considered rays at the center of the FOV. What happens as we move toward the edges of the array?
 - The rays strike the aperture at a glancing angle and are asymmetrically deviated
 - Coma and astigmatism will be large
 - In this case, aberration would be reduced by moving the detector much closer to the lens



The symmetry has been broken by the aperture. Will this optical system really work?

18

Geometry I gives an awful MTF result off axis. The straight rays are blocked, and the ones that are permitted are sharply bent, leading to significant aberration.

IDA Calculation: Geometry II

- For the conditions specified in the Stanford paper, the IDA model gives comparable but somewhat less optimistic results:

F# = 3.5: Identical to Stanford

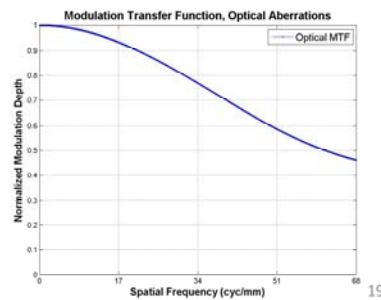
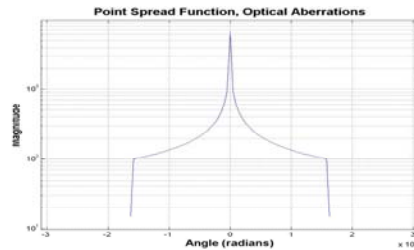
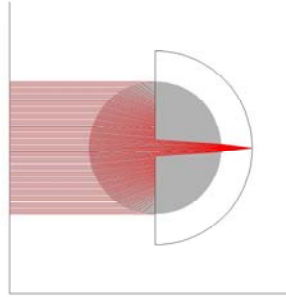
Lens radius = 4 mm: Identical to Stanford

$n_{\text{LENS}} = 1.5168$ (n_d for BK-7 glass): Stanford used a weighted sum of the response at Fraunhofer lines C (H), F (H), and d (He)

$n_c = 1.51432$, $n_f = 1.52238$, $n_d = 1.51680$

Detector radius (and position) = 5.87 mm: Identical to Stanford. Note that this is the focal length of the lens (at n_d)

Diagram of Optical System and Detector



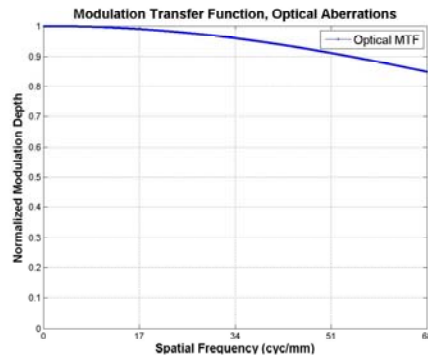
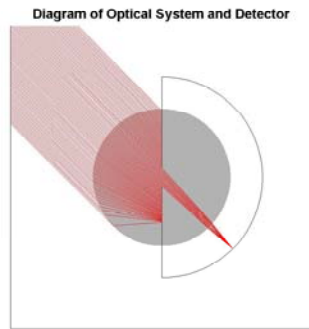
The Stanford paper shows an MTF of about 0.6 (~0.75 of the diffraction limit) at 68 cyc/mm. Our computation yielded an MTF of 0.47 at 68 cyc/mm.

Geometry II does slightly better than Geometry I, although the MTF is still not as high as that shown in the Stanford paper.

The difference between Geometry I and Geometry II on axis is only because of the differences in f# definition.

Geometry II: Off-Axis Behavior

- What happens as we move toward the edges of the array?
 - The projection of the hole appears smaller at 45 deg
 - PSF narrows, so MTF improves (at the cost of a decrease in signal strength)



This is an enormous improvement over Geometry I!
In fact, it is even better than the on-axis performance for either geometry

20

Geometry II preserves (and even improves) the MTF off axis.

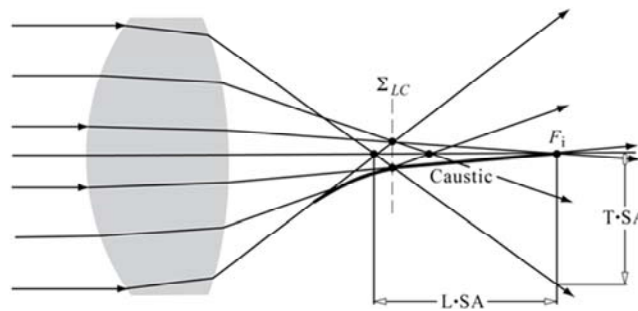
Adjustment of Detector Position

Geometry II is clearly the better way forward. However, two questions remain:

- Why are the published MTFs, which presumably include diffraction, higher than ours?
- Are there any simple adjustments we can make to increase our MTFs?

Also, the focal position is a sub-optimal location for the detector

- In a spherically aberrated converging optical system, some benefit is gained in moving the detector slightly closer to the lens than the focal position. The optimal point trades focal precision of rays nearest the center of the entrance pupil for minimization of total blur spot area (circle of least confusion)



The circle of least confusion occurs where the marginal rays exit the caustic envelope. This occurs at the location Σ_{LC} in the figure*

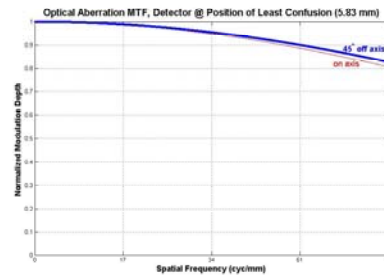
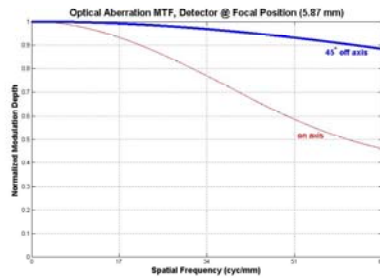
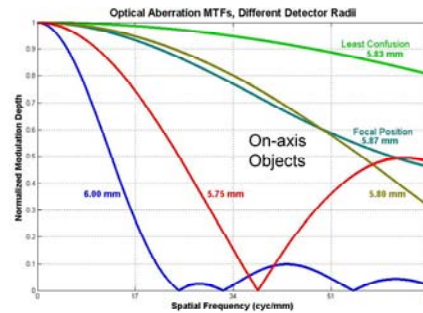
* Figure from Eugene Hecht, *Optics*, 3rd ed. (Reading, MA: Addison Wesley Publishing Company, 1997) 21

The circle of least confusion is the position where the image plane (detector) should be placed to minimize the overall size of the aberration blur spot. For a converging lens with positive longitudinal spherical aberration (LSA), as is the case here, this position will be located in front of the focal position. Assuming axial symmetry, the circle of least confusion is defined as the locus of points where a marginal ray exits the caustic ray bundle (envelope).

Optimal Detector Position

MTF improves significantly when the detector is placed at the position of least confusion

This placement improves the overall MTF and greatly reduces its dependence on object position



22

By changing the position of the FPA, we can get a variety of MTF results. For the focal position at 5.87 mm, which was the position used by the Stanford Group, we compute about 0.47 for the MTF at 68 cyc/mm. The position at 5.83 mm (circle of least confusion) gives 0.8 for the MTF at 68 cyc/mm—a much better result.

The two charts at the bottom of this slide show how the dependence of MTF upon object angle is also diminished by moving to the circle of least confusion.

Possible Enhancements

The following considerations, while not mentioned by the authors, might also be useful:

1. Could the lens be *coated* with a material that would *transmit rays near normal* incidence but would strongly reflect radiation at other angles?
2. Could a spherically symmetric *GRIN* lens allow a wider aperture?
3. Could the detector position (and size) be optimized further, in combination with Options 1 and 2?

Conclusions

We have demonstrated that the proposed optical system could lead to consistent resolution across a wide FOV

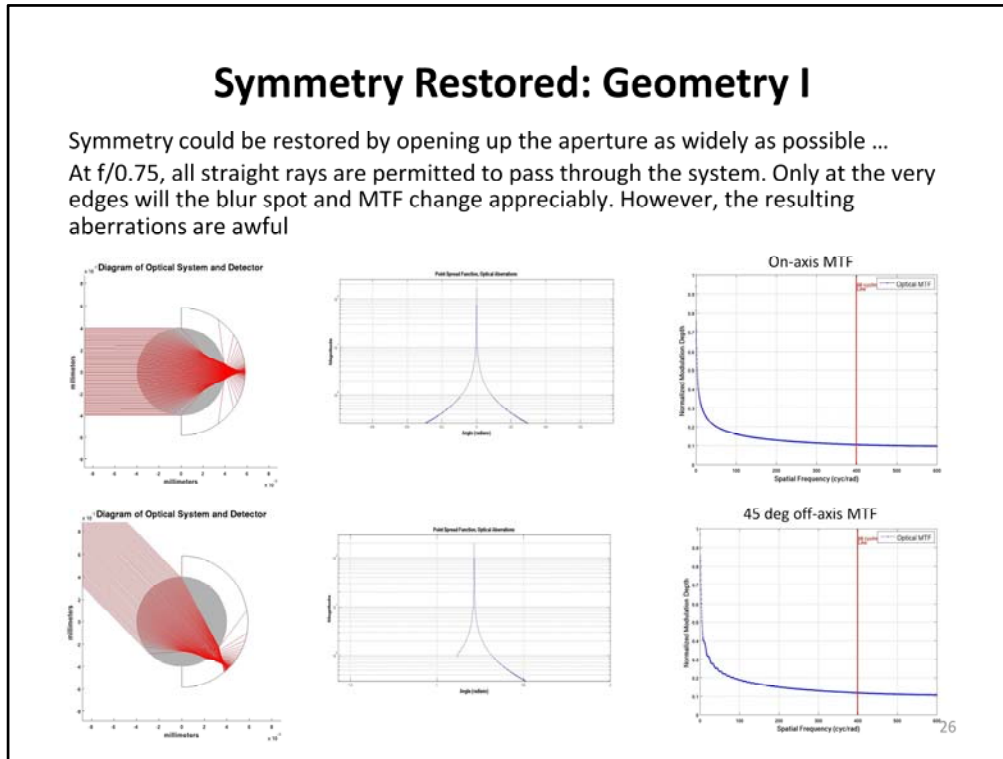
The ideal location for the detector is not the focal position but the position of least confusion

The requirement for an aperture (for a reasonable blur spot) breaks the spherical symmetry alluded to in the Stanford paper, but the effect on MTF is small at the position of least confusion

Backup

Symmetry Restored: Geometry I

Symmetry could be restored by opening up the aperture as widely as possible ...
At $f/0.75$, all straight rays are permitted to pass through the system. Only at the very edges will the blur spot and MTF change appreciably. However, the resulting aberrations are awful

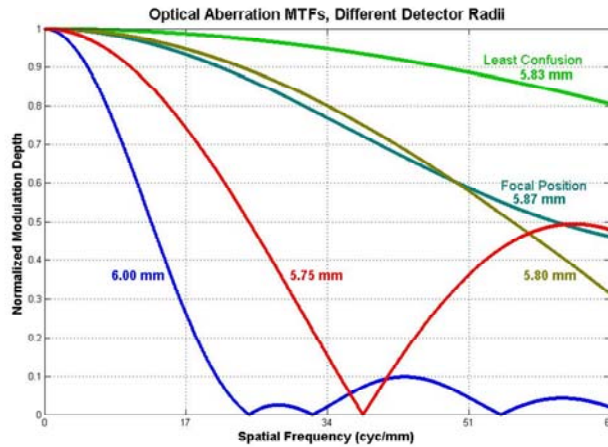


We initially investigated the authors' symmetry claims with Geometry I and found results that disagreed strongly. The reason for the discrepancy was that the insertion of an aperture had broken the spherical symmetry that was purported to ensure that the image resolution would not deteriorate as the object moved off axis toward the edges of the FOV.

Here, we note that by eliminating the Geometry I aperture, we can preserve the spherical symmetry. However, the aberrations now dominate, and the results are poor.

Optimal Detector Position

- We found that these results are very sensitive to detector position
 - Some benefit is gained in moving the detector slightly closer to the lens than the 5.87-mm focal position. The optimal point trades the focal precision of rays nearest the center of the entrance pupil for the minimization of total blur spot area (circle of least confusion)

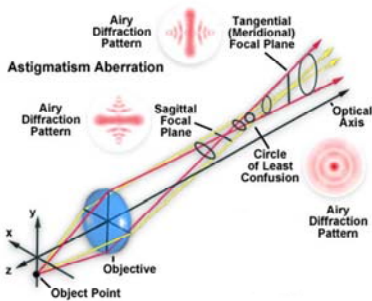


27

By changing the position of the FPA, we can get a variety of MTF results. The position at 5.87 mm, which was used by the Stanford Group, gives about 0.47 for the MTF at 68 cyc/mm. The position at 5.83 mm (circle of least confusion) gives 0.8 for the MTF at 68 cyc/mm—a much better result.

Circle of Least Confusion

Light rays lying in the tangential and sagittal planes are refracted differently and both sets of rays intersect the chief ray at different image points, termed the tangential line image (tangential focal plane) and the sagittal line image (sagittal focal plane). These rays fail to produce a focused image point; rather, they produce a series of elongated images ranging from linear to elliptical, depending upon the position within the optical train. In a zone known as the **circle of least confusion** (positioned between the tangential line image and the sagittal line image), the major and minor axes of the ellipse are equal and the image approaches a circular geometry



Source: <http://micro.magnet.fsu.edu/primer/java/aberrations/astigmatism/index.html>

28

The circle of least confusion is the smallest image (blur patch of light) of point source that optical system can project. As lens moves in and out of focus, patch of light grows and decreases in size. The smallest size is circle of least confusion, and the optical system is said to be in focus. Note: due to the wave nature of light and depending on lens design, the circle of least confusion does not necessarily give best definition (Source: http://www.idigitalphoto.com/dictionary/circle_of_least_confusion.)

Appendix A. Ray Tracing Codes

Analytical Modulation Transfer Function (MTF) Calculation

In the process of developing the main ray tracing code for our general use, we decided that we needed a simple closed form result to check our numerical results. This would provide assurance that the code was dependable—at least for simple functions.

This is the closed-form solution used to calculate the MTF for simple functions (i.e., sine with (1) varying spatial frequency as the object and (2) Gaussian of various widths as the point spread function (PSF)). This result was used to check the MATLAB code RAYMTF and gain confidence in the RAYMTF code's MTF results for more complex systems.

We start with two functions: a sine wave with frequency f , $\text{Sin}(fx)$, and a Gaussian with parameter, e^{-ax^2} , as the impulse response. The parameter “ a ” is related to the typical width of the Gaussian by the relationship $= \frac{1}{4\sigma^2}$.

The first step is to do the convolution of the two functions:

$$\int dx \text{Sin}(fx)e^{-a(x-t)^2}. \quad (\text{A-1})$$

To facilitate the calculation, the exponential description of the sine is used:

$$\begin{aligned} \frac{1}{2i} \int dx (e^{+ifx} - e^{-ifx})e^{-a(x-t)^2} &= \frac{1}{2i} \int dx (e^{+ifx-a(x-t)^2} - e^{-ifx-a(x-t)^2}) \\ &= \frac{1}{2i} \int dx (e^{-ax^2-(2at-if)x-at^2} - e^{-ax^2-(2at+if)x-at^2}). \end{aligned} \quad (\text{A-2})$$

Focusing on the first term, we can solve it by completing the square to get a shifted Gaussian and a constant exponential:

$$\begin{aligned} -ax^2 - (2at - if)x - at^2 &= -a \left[x^2 - 2 \left(t + i \frac{f}{2a} \right) x + t^2 \right] \\ &= -a \left[x^2 - 2 \left(t + i \frac{f}{2a} \right) x + \left(t + i \frac{f}{2a} \right)^2 - \left(t + i \frac{f}{2a} \right)^2 + t^2 \right] \\ &= -a \left[\left(x - \left(t + i \frac{f}{2a} \right) \right)^2 - \left(t^2 + \frac{ift}{a} - \frac{f^2}{4a^2} \right) + t^2 \right] \\ &= -a \left(x - \left[t + i \frac{f}{2a} \right] \right)^2 + \left(+ift - \frac{f^2}{4a} \right). \end{aligned} \quad (\text{A-3})$$

Going back to the integral, we get

$$\int \frac{dx}{2i} e^{-a(x-[t+i\frac{f}{2a}])^2} e^{+ift-f^2/4a}. \quad (\text{A-5})$$

The only difference between the first and second terms is the sign of the complex term, ift , so by making the substitution in the previous calculation of

$$+ift \rightarrow -ift, \quad (\text{A-6})$$

we get for the second term

$$\int \frac{dx}{2i} e^{-a(x-[t-i\frac{f}{2a}])^2} e^{-ift-f^2/4a}. \quad (\text{A-7})$$

The two terms can now be put together (the Gaussian integral calculated and constant terms rearranged) to get

$$\sqrt{\frac{\pi}{a}} e^{-f^2/4a} \frac{(e^{+ift} - e^{-ift})}{-2i}. \quad (\text{A-8})$$

To get the MTF, we divide by the original function, $Sin(ft)$, to get

$$MTF(f, a) = \sqrt{\frac{\pi}{a}} e^{-f^2/4a}. \quad (\text{A-9})$$

To relate back to the original width of the Gaussian, we use the relationship $a = \frac{1}{4\sigma^2}$:

$$MTF(f, \sigma) = \sqrt{\frac{\pi}{a}} e^{-(f\sigma)^2}. \quad (\text{A-10})$$

(This space intentionally left blank.)

MTFCHECK1

This is the “Mathematica” code used to graph the analytical MTF results.

```

F[x_, f_] := Sin[f x / (2 Pi)];
G[x_, a_] := Sqrt[Pi / a] Exp[-a x^2];

F[x, f]

Sin[ $\frac{f x}{2 \pi}$ ]

G[x, a]

 $\sqrt{\frac{1}{a} e^{-a x^2} \sqrt{\pi}}$ 

Convolve[Sin[f x / (2 Pi)], Sqrt[Pi / a] Exp[-a x^2], x, y]

$Aborted

F[x, f]

Sin[ $\frac{f x}{2 \pi}$ ]

f = 2; a = 1;

F[x, f]

Sin[ $\frac{x}{\pi}$ ]

Convolve[x, 1 / (x^2 + 1), x, y]

 $\pi y$ 

Convolve[Sin[ff x], E^(-a x^2), x, y]

 $-\frac{1}{2} i e^{-\frac{1}{4} ff (ff+4 i y)} (-1 + e^{2 i ff y}) \sqrt{\pi}$ 

h[y_] :=  $-\frac{1}{2} i e^{-\frac{1}{4} ff (ff+4 i y)} (-1 + e^{2 i ff y}) \sqrt{\pi}$ 

ComplexExpand[h[y]]

 $\frac{1}{2} e^{-\frac{ff^2}{4}} \sqrt{\pi} \sin[ff y] - \frac{1}{2} e^{-\frac{ff^2}{4}} \sqrt{\pi} \cos[2 ff y] \sin[ff y] + \frac{1}{2} e^{-\frac{ff^2}{4}} \sqrt{\pi} \cos[ff y] \sin[2 ff y] +$ 
 $i \left( \frac{1}{2} e^{-\frac{ff^2}{4}} \sqrt{\pi} \cos[ff y] - \frac{1}{2} e^{-\frac{ff^2}{4}} \sqrt{\pi} \cos[ff y] \cos[2 ff y] - \frac{1}{2} e^{-\frac{ff^2}{4}} \sqrt{\pi} \sin[ff y] \sin[2 ff y] \right)$ 

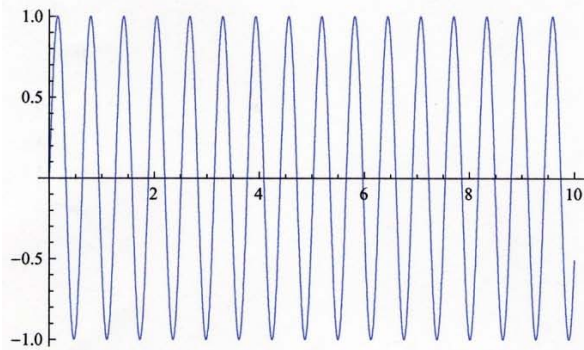
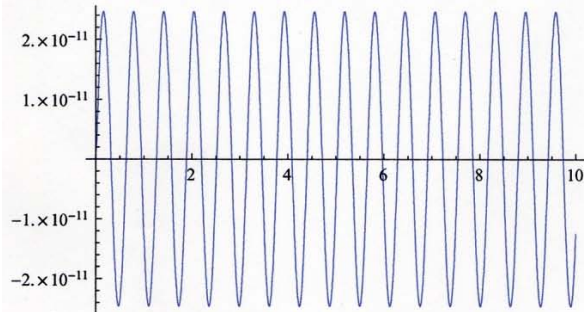
```

ComplexExpand[h[y] / Sin[ff y]]

$$\begin{aligned}
 & \frac{e^{-\frac{ff^2}{4}} \sqrt{\pi} \sin[ff y]^2}{-1 + \cos[2 ff y]} + \frac{e^{-\frac{ff^2}{4}} \sqrt{\pi} \cos[2 ff y] \sin[ff y]^2}{-1 + \cos[2 ff y]} - \\
 & \frac{e^{-\frac{ff^2}{4}} \sqrt{\pi} \cos[ff y] \sin[ff y] \sin[2 ff y]}{-1 + \cos[2 ff y]} + i \left(-\frac{e^{-\frac{ff^2}{4}} \sqrt{\pi} \cos[ff y] \sin[ff y]}{-1 + \cos[2 ff y]} + \right. \\
 & \left. \frac{e^{-\frac{ff^2}{4}} \sqrt{\pi} \cos[ff y] \cos[2 ff y] \sin[ff y]}{-1 + \cos[2 ff y]} + \frac{e^{-\frac{ff^2}{4}} \sqrt{\pi} \sin[ff y]^2 \sin[2 ff y]}{-1 + \cos[2 ff y]} \right)
 \end{aligned}$$

Plot[(h[y]) /. (ff -> 10), {y, 0, 10}]

Plot[(Sin[ff y]) /. (ff -> 10), {y, 0, 10}]



ExpToTrig[h[y] / Sin[ff y]]

$$-\frac{1}{2} i \sqrt{\pi} \csc[ff y] (-1 + \cos[2 ff y] + i \sin[2 ff y]) \left(\cosh\left[\frac{1}{4} ff (ff + 4 i y)\right] - \sinh\left[\frac{1}{4} ff (ff + 4 i y)\right] \right)$$

a = 1

1

Convolve[Sin[f x], E^(-b x^2), x, y, Assumptions -> b > 0] / (Sin[f y])

$$\frac{i e^{-\frac{f(f+4ib y)}{4b}} \sqrt{\pi} \csc[f y] \left(-2 + 2 e^{2 i f y} + \operatorname{Erf}\left[\frac{-i f + 2 b y}{2 \sqrt{b}}\right] + i \operatorname{Erfi}\left[\frac{f + 2 i b y}{2 \sqrt{b}}\right] \right)}{4 \sqrt{b}}$$

$$\text{ExpToTrig}\left[\frac{i e^{-\frac{f(f+4ib)y}{4b}} \sqrt{\pi} \text{Csc}[fy] \left(-2 + 2 e^{2if y} + \text{Erf}\left[\frac{-if+2by}{2\sqrt{b}}\right] + i \text{Erfi}\left[\frac{f+2iby}{2\sqrt{b}}\right]\right)}{4\sqrt{b}}\right]$$

$$\frac{1}{4\sqrt{b}}$$

$$i \sqrt{\pi} \text{Csc}[fy] \left(-2 + 2 \text{Cos}[2fy] + \text{Erf}\left[-\frac{if}{2\sqrt{b}} + \sqrt{b} y\right] + i \text{Erfi}\left[\frac{f}{2\sqrt{b}} + i \sqrt{b} y\right] + 2i \text{Sin}[2fy]\right) \left(\text{Cosh}\left[\frac{f(f+4iby)}{4b}\right] - \text{Sinh}\left[\frac{f(f+4iby)}{4b}\right]\right)$$

`Simplify[%, f > 0 && b > 0 && Element[b, Reals]]`

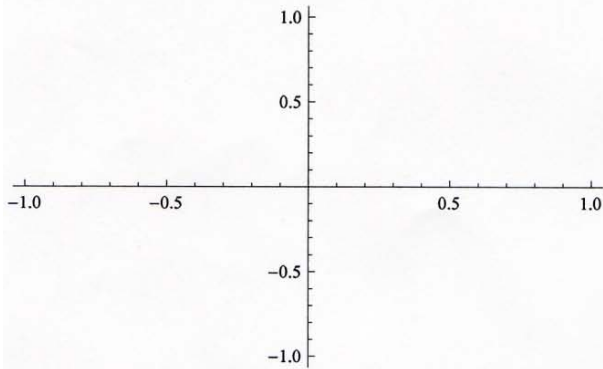
$$\frac{1}{4\sqrt{b}} i \sqrt{\pi} \text{Csc}[fy] \left(-2 + 2 \text{Cos}[2fy] + \text{Erf}\left[\frac{-if+2by}{2\sqrt{b}}\right] + i \text{Erfi}\left[\frac{f+2iby}{2\sqrt{b}}\right] + 2i \text{Sin}[2fy]\right) \left(\text{Cosh}\left[\frac{f(f+4iby)}{4b}\right] - \text{Sinh}\left[\frac{f(f+4iby)}{4b}\right]\right)$$

`Simplify[`

$$\frac{1}{4\sqrt{b}} i e^{-\frac{f(f+4iby)}{4b}} \sqrt{\pi} \text{Csc}[fy] \left(-2 + 2 e^{2if y} + \text{Erf}\left[\frac{-if+2by}{2\sqrt{b}}\right] + i \text{Erfi}\left[\frac{f+2iby}{2\sqrt{b}}\right]\right) /. b \rightarrow 5]$$

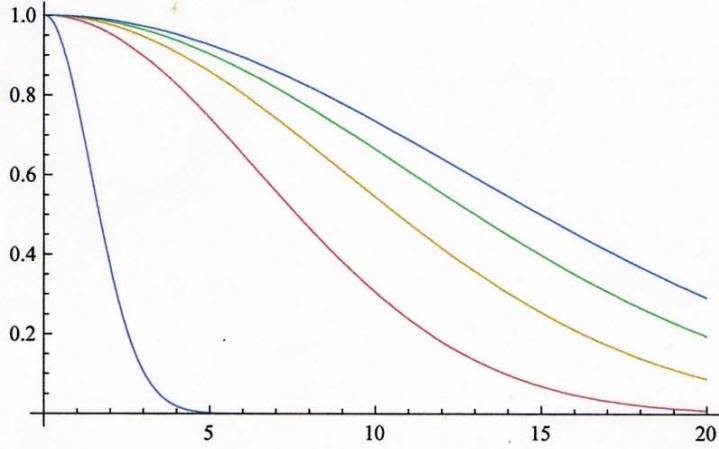
$$-e^{-\frac{f^2}{20}} \sqrt{\frac{\pi}{5}}$$

`Plot` $\left[\left[\frac{1}{4\sqrt{b}} i e^{-\frac{f(f+4iby)}{4b}} \sqrt{\pi} \text{Csc}[fy] \left(-2 + 2 e^{2if y} + \text{Erf}\left[\frac{-if+2by}{2\sqrt{b}}\right] + i \text{Erfi}\left[\frac{f+2iby}{2\sqrt{b}}\right]\right)\right] /. b \rightarrow 1, \{f, 0, 100\}, \text{PlotRange} \rightarrow \text{All}]\right]$

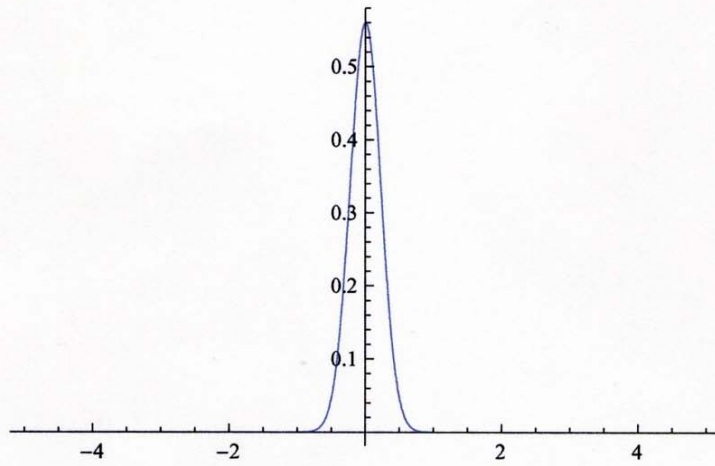


`MFT1[f_, b_] := e-f2/4b`

```
Plot[Evaluate[Table[MFT1[f, b], {b, 1, 100, 20}], {f, 0, 20}, PlotRange -> All]
```



```
Plot[Sqrt[Pi / a] E^(-a x^2), {x, -5, 5}, PlotRange -> All]
```



```
Convolve[HeavisidePi[x], Sin[x], x, y]
```

```
Convolve[HeavisidePi[x], Sin[x], x, y]
```

(This space intentionally left blank.)

MTFCHECK2

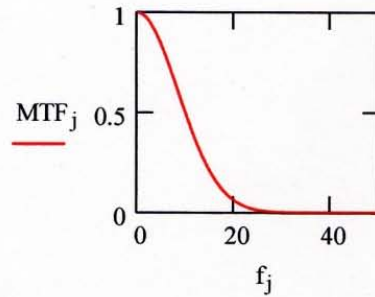
This is the "MATHCAD" code used to graph the analytical MTF results.

$$\Delta f := 0.1 \quad f_0 := 0.1 \quad j := 1, 2.. 700$$

$$f_j := f_0 + \Delta f \cdot j \quad \alpha := 0.007$$

$$MTF_j := e^{-\alpha \cdot (f_j)^2}$$

a



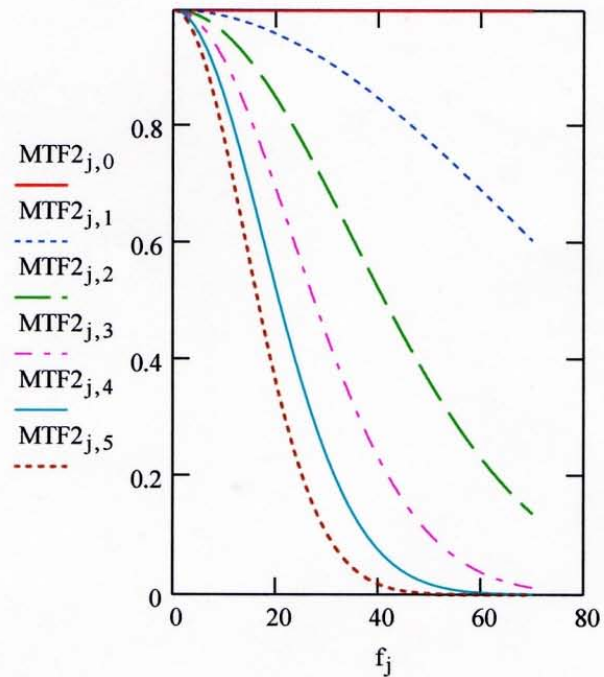
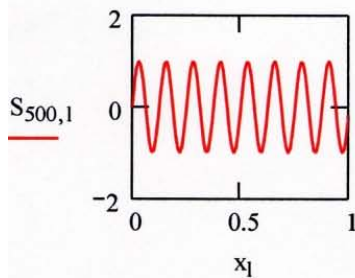
$$\Delta \sigma := 0.01 \quad \sigma_0 := 0.0001 \quad k := 0, 1.. 10 \quad \Delta x := 0.01$$

$$\sigma_k := \sigma_0 + \Delta \sigma \cdot k \quad l := 0, 1.. 100 \quad m := 1, 2.. 10$$

$$x_l := \Delta x \cdot l$$

$$MTF2_{j,k} := e^{-(f_j)^2 \cdot (\sigma_k)^2}$$

$$S_{j,l} := \sin(f_j \cdot x_l)$$



$$c_0 := 0.00001 \quad \Delta a := 0.1 \quad a_0 := 0.0001$$

$$\Delta c := 0.002$$

$$c_m := c_0 + \Delta c \cdot m \quad a_m := a_0 + \Delta a \cdot m$$

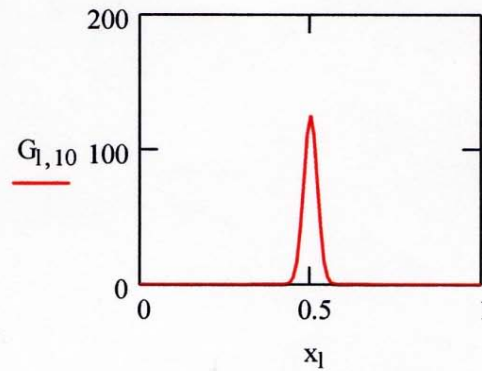
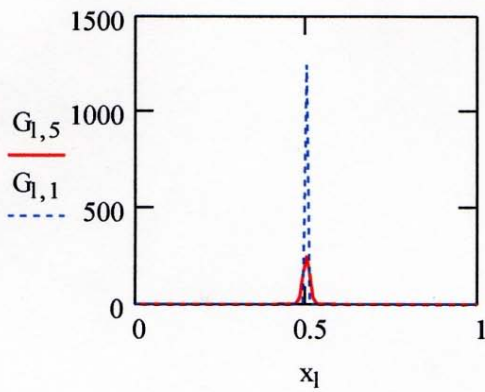
$$x_1 = 0.01$$

$$G_{1,m} := \sqrt{\pi \div a_m} e^{-a_m \cdot ((0.5-x_1))^2}$$

$$a_5 = 0.5$$

$$G_{1,m} := \left(1 \div c_m \cdot \sqrt{2 \cdot \pi}\right) e^{-\frac{(0.5-x_1)^2}{2 \cdot (c_m)^2}}$$

$$\sigma_5 = 0.05$$



(This space intentionally left blank.)

RAYMTF

This is the MATLAB code used to calculate the ray tracing results and the MTFs and PSFs shown in Chapter 4.

```
% rek 20110120
%to do: flat fpa
%to do: thin lens
%to do: compound optics
%to do: allow multiple wavelengths... (dispersion)

% 1) INPUT PARAMETERS:
% 1a) SCENARIO:
    numObjectPoints = 1;
    objectPoints_definedbyPolarCoords = true;
        objectAngles = 180*pi/180; % radians % (if using POLAR Coords)
            % measured from +x axis (row vector of ObjAngles, one per
ObjPoint)
        objectDistance = 1000; % meters % (if using POLAR Coords)
            % if very big compared to sensor size, incoming
rays will be parallel
        objectPoints__CartesianDefault = [-1e3;0]; % meters % (if not using
POLAR Coords)
% 1b) SENSOR PARAMETERS:
% 1b1) optical elements:
    lensRadius = 0.004; % meters
    lensCenter = [0;0]; % meters % Cartesian coordinates of lens center
    nLens = 1.5168; %index of refraction n_D3 (i.e. at yellow Helium line at 587.6 nm)
        % note that Stanford weighted their design, analysis and results
for n_C, n_D3, and n_F:
        % weights = {1,2,1}
        % according to http://refractiveindex.info/?
group=GLASSES&material=BK7
        % n_C = 1.51432 @ 656.3 nm
        % n_D3 (= n_d) = 1.5168 @ 587.6 nm
        % n_F = 1.52238 @ 486.1 nm

    nAir = 1; %index of refraction for surrounding medium
% 1b2) aperture stops:
    useFnumberinput_toCalculateFrontsideAperture = true; % Geometry I: aperture at
front of lens
        frontsideAp__fNumber = 0; % Geometry I (if using
fNumber input)
        frontsideApertureRadius__default = lensRadius; % Geometry I (if not
using fNumber input)
    useFnumberinput_toCalculateInsideAperture = true; % Geometry II: aperture
inside lens
        insideAp__fNumber = 3.5; % Geometry II (if using
fNumber input)
        insideApertureRadius__default = lensRadius; % Geometry II (if not
using fNumber input)
% 1b3) detector:
    fpaCenter = [0;0]; % Cartesian coordinates of fpa center
    putFPAatFocalPosition = false;
        designobjectDistance = Inf; %ObjDist which determines FPA position (use lens
maker's eqn).
    putFPAatCircleOfLeastConfusion = false;
```

```

hardwireFPAposition = not(putFPAatFocalPosition || putFPAatCircleOfLeastConfusion);
detectorRadius = 0.00583; % meters % (only used if hardwiring FPA
position)
% 1c) PRECISION of Calculation (and Charts):
numRays_perObjectPoint = 10000; %number of evenly spaced meridional rays to draw from
the object to the lens
nPSF_sampleBins = 65536; %the number of bins with which to sample the optical point
spread function
maxPlot = 105; %limit for number of rays to plot
pixWidth = pi/1000; %angular size of pixel used for computing detector MTF (radians)
% End input parameters

% 2) GET CONFIG INFO (Get All Configuration Info from Input Parameters):
% 2a) object Points:
if (objectPoints_definedbyPolarCoords)
objectPoints = objectDistance*[cos(objectAngles);sin(objectAngles)]; %coordinates of
point sources
else
objectPoints = objectPoints__CartesianDefault;
end
% 2b) focal position:
focalRadius_ord1 = 1/((2*(nLens-1))/(nLens*lensRadius)-1/designobjectDistance);
%lens makers equation (focuses objects at "designobjectDistance")
FIRST ORDER !
% 2c1) front aperture:
if (useFNumberinput_toCalculateFrontsideAperture)
% see comments on 'useFNumberinput_toCalculateInsideAperture' below!
fNumber = frontsideAp__fNumber;
% solve for y_exitpupil using quadratic formula:
a = 1 + 4*fNumber*fNumber;
b = -4*fNumber*focalRadius_ord1;
c = (focalRadius_ord1.^2) - (lensRadius.^2);
discriminant = b.^2-4*a.*c;
if (discriminant<=0)
% if this fNumber defines an exit cone that either misses the lens or is tangent
to it:
frontsideApertureRadius = lensRadius;
yMarginal__exitPupil = NaN;
xMarginal__exitPupil = NaN;
yMarginal__entrancePupil = NaN;
xMarginal__entrancePupil = NaN;
else
temp = (-b-sqrt(discriminant))./(2*a); % smallest root will be the correct
answer here.
yMarginal__exitPupil = temp;
xMarginal__exitPupil = focalRadius_ord1 - 2*fNumber*yMarginal__exitPupil;
% solve for refracted angle at exit cone:
exitRayDirection = atan(-1/(2*fNumber));
direction_radial_to_exitPoint=atan((yMarginal__exitPupil-lensCenter(2)) ...

```



```

a = 1 + 4*fNumber*fNumber;
b = -4*fNumber*focalRadius_ord1;
c = (focalRadius_ord1.^2) - (lensRadius.^2);
discriminant = b.^2-4*a.*c;
if (discriminant<=0)
    % if this fNumber defines an exit cone that either misses the lens or is tangent ✓
to it:
    insideApertureRadius = lensRadius;
    yMarginal__exitPupil = NaN;
    xMarginal__exitPupil = NaN;
    yMarginal__entrancePupil = NaN;
    xMarginal__entrancePupil = NaN;
else
    temp = (-b-sqrt(discriminant))./(2*a);          % smallest root will be the correct ✓
answer here.
    yMarginal__exitPupil = temp;
    xMarginal__exitPupil = focalRadius_ord1 - 2*fNumber*yMarginal__exitPupil;
    % solve for refracted angle at exit cone:
    exitRayDirection = atan(-1/(2*fNumber));
    direction_radial_to_exitPoint=atan((yMarginal__exitPupil-lensCenter(2)) ...
                                        / (xMarginal__exitPupil-lensCenter
(1)));
    refractedAngle = direction_radial_to_exitPoint - exitRayDirection;
    incidentAngle = asin((nAir/nLens)*sin(refractedAngle)); % still going ✓
backwards...
    internalRayDirection2 = direction_radial_to_exitPoint - incidentAngle;
    yMarginalIntercept = yMarginal__exitPupil + ...
                        ((lensCenter(1)-xMarginal__exitPupil)*(tan
(internalRayDirection2)));
    insideApertureRadius = yMarginalIntercept;
end %
    insideAp__entrancePupil = [xMarginal__entrancePupil;yMarginal__entrancePupil];
    insideAp__exitPupil = [xMarginal__exitPupil;yMarginal__exitPupil];
else
    % placeholder, insert default calc here.
end
    % 2d) detector position:
if (putFPAatFocalPosition)
    detectorRadius = focalRadius_ord1;
end
if (putFPAatCircleOfLeastConfusion)
    % placeholder, havent done this calculation yet...
end

% 3) RAY TRACING:
    % 3a) rays from object to lens entrance: (objectPoints->lensEnterPoints):
%create lens points (points on the lens through which rays can pass)

```

```

lensCenter2Object = objectPoints-repmat(lensCenter,1,numObjectPoints);
lensCenter2ObjectDistance = sqrt(sum(lensCenter2Object.^2,1));
objectAngleMax = asin(lensRadius./lensCenter2ObjectDistance);
lensObjectAngle = atan2(lensCenter2Object(2,:)./lensCenter2ObjectDistance,...
    lensCenter2Object(1,:)./lensCenter2ObjectDistance);
index = zeros(1,numRays_perObjectPoint*numObjectPoints);
lensAngles = zeros(1,numRays_perObjectPoint*numObjectPoints);
for objectIndex = 1:numObjectPoints
    angleOffsets = linspace(-objectAngleMax(objectIndex),objectAngleMax(objectIndex),
numRays_perObjectPoint);
    relativeLensAngle = -abs(angleOffsets)+...
        asin((lensCenter2ObjectDistance(objectIndex)/lensRadius)*sin
(abs(angleOffsets)));
    newLensAngles = lensObjectAngle(objectIndex)-sign(angleOffsets).*relativeLensAngle;
    index((numRays_perObjectPoint*(objectIndex-1)+1):
(numRays_perObjectPoint*objectIndex)) = ...
        repmat(objectIndex,1,numel
(newLensAngles));
    lensAngles((numRays_perObjectPoint*(objectIndex-1)+1):
(numRays_perObjectPoint*objectIndex)) = ...
        newLensAngles;
end
lensAngles(lensAngles<0) = 2*pi-abs(lensAngles(lensAngles<0));
angles = lensAngles;
nLensEnterPoints = numel(angles);
lensEnterPoints = repmat(lensCenter,1,nLensEnterPoints) + lensRadius*[cos(angles);sin
(angles)];
% ad hoc fix to block the points that hit detector box before lens:
lensEnterPointsOnWrongSide = (lensEnterPoints(1,:) > 0);
lensEnterPoints(:,lensEnterPointsOnWrongSide) = NaN;
%create unit rays from object points to lens points
objectIndex = index;
obj2Lens = lensEnterPoints-objectPoints(:,objectIndex);
unitObj2Lens = obj2Lens./repmat(sqrt(sum(obj2Lens.^2,1)),2,1);

    % 3b) entry refraction:
lensNormals = lensEnterPoints-repmat(lensCenter,1,nLensEnterPoints);
lensNormals = lensNormals./repmat(sqrt(sum(lensNormals.^2,1)),2,1);
incidentAngle = acos(sum(lensNormals.*-unitObj2Lens,1));
angleSign = sign(-unitObj2Lens(1,:).*lensNormals(2,:) - -unitObj2Lens(2,:).*lensNormals
(1,:));
incidentAngle = incidentAngle.*angleSign; % need to get the orientation right
refractionAngle = asin(nAir/nLens*sin(incidentAngle));
frontside_validIndex = abs(lensAngles-pi)<frontside_Ap_Angle/2;
refractionAngle(~frontside_validIndex) = NaN;
%calculate deflected rays
deflectionAngle = refractionAngle-incidentAngle;
R11 = cos(deflectionAngle);
R12 = sin(deflectionAngle);
R21 = -R12;
R22 = R11;

```

```

lensRayDirection = [R11.*unitObj2Lens(1,:)+R12.*unitObj2Lens(2,:);R21.*unitObj2Lens(1,:)
+R22.*unitObj2Lens(2,:)]

    % 3c) rays inside lens: (lensEnterPoints->lensExitPoints):
%calculate hypothetical lens exit points (if they get past the inner aperture!)
temp = -2*(sum(lensEnterPoints.*lensRayDirection,1)-...
    sum(repmat(lensCenter,1,nLensEnterPoints).*lensRayDirection,1));
lensExitPoints = lensEnterPoints + repmat(temp,2,1).*lensRayDirection;
lensEnter_x = lensEnterPoints(1,:);
lensEnter_y = lensEnterPoints(2,:);
lensExit_x = lensExitPoints(1,:);
lensExit_y = lensExitPoints(2,:);
yIntercept_PassingLensCenter = (((lensExit_x.*lensEnter_y)-(lensEnter_x.*lensExit_y))./(
lensExit_x-lensEnter_x));
validindex_yInterceptCenter = ((abs(yIntercept_PassingLensCenter))
<insideApertureRadius);
lensExitPoints(:,~validindex_yInterceptCenter) = NaN;

    % 3d) exit refraction:
lensNormals = repmat(lensCenter,1,nLensEnterPoints)-lensExitPoints;
lensNormals = lensNormals./repmat(sqrt(sum(lensNormals.^2,1)),2,1);
unitExitRays = lensEnterPoints-lensExitPoints;
unitExitRays = -unitExitRays./repmat(sqrt(sum(unitExitRays.^2,1)),2,1);
exitAngle = acos(sum(-unitExitRays.*lensNormals,1));
angleSign = sign(-unitExitRays(1,:).*lensNormals(2,:) - -unitExitRays(2,:).*lensNormals
(1,:));
exitAngle = angleSign.*exitAngle;
refractionAngle = asin(nLens/nAir*sin(exitAngle));
%calculate deflected rays
deflectionAngle = refractionAngle-exitAngle;
R11 = cos(deflectionAngle);
R12 = sin(deflectionAngle);
R21 = -R12;
R22 = R11;
exitRayDirection = [R11.*unitExitRays(1,:)+R12.*unitExitRays(2,:);R21.*unitExitRays(1,:)
+R22.*unitExitRays(2,:)]

    % 3e) rays from lens exit to detector: (lensExitPoints->fpaPoints):
%calculate focal plane entry points
a = 1;
b = 2*sum(exitRayDirection.*(lensExitPoints-repmat(fpaCenter,1,nLensEnterPoints)),1);
c = sum((lensExitPoints-repmat(fpaCenter,1,nLensEnterPoints)).^2,1)-detectorRadius^2;
temp = (-b+sqrt(b.^2-4*a.*c))./(2*a);
fpaPoints = lensExitPoints + repmat(temp,2,1).*exitRayDirection;

% 4) PLOT AND SAVE FIGURES:
    % 4a) make name tag:
nFloor = num2str(floor(nLens));

```

```

nFrac = num2str(nLens-floor(nLens),'%6.4f');
clipname = ['zNO_n',nFloor,'p',nFrac(3:end),'_ap',num2str(floor(
(frontside_Ap_Angle*180/pi)),'_f',...
            num2str(floor(detectorRadius*10^6)),...
            '_oA',num2str(floor(objectAngles*180/pi)),'_'];

% 4b) plot ray trace:
% 4b1) lens, detector, and object:
figure;
set(gcf,'ToolBar','figure');
set(gcf,'OuterPosition',outerPosition__full_figure())
set(gcf,'Position',position__full_figure())
pause on
pause(1)
hold on
axis equal
%plot lens
dAngle = pi/100;
angle = 0:dAngle:2*pi;
nPts = numel(angle);
points = repmat(lensCenter,1,nPts) + lensRadius*[cos(angle);sin(angle)];
%plot(points(1,:),points(2,:))
patch(points(1,:),points(2,:),[0.7,0.7,0.7],'EdgeColor','none')
plot([0,0],[-detectorRadius,-insideApertureRadius],'k')
plot([0,0],[detectorRadius,insideApertureRadius],'k')
angle = linspace(frontside_Ap_Angle/2,pi/2,300);
nPts = numel(angle);
points = repmat(lensCenter,1,nPts) + lensRadius*[-cos(angle);sin(angle)];
plot(points(1,:),points(2:),'k')
points = repmat(lensCenter,1,nPts) + lensRadius*[-cos(angle);-sin(angle)];
plot(points(1,:),points(2:),'k')
%plot fpa
dAngle = pi/100;
angle = -pi/2:dAngle:pi/2;
nPts = numel(angle);
points = repmat(fpaCenter,1,nPts)+detectorRadius*[cos(angle);sin(angle)];
plot(points(1,:),points(2:),'k')
%plot object points
plot(objectPoints(1,:),objectPoints(2:),'bo')
% 4b2) rays:
%plot rays from object points to lens
start = objectPoints(:,objectIndex);
stop = start + obj2Lens;
% AD HOC FIX FOR THE RAYS PASSING THE FPA GUARD LINE !!!!!:
x = [start(1,:);stop(1,:)];
y = [start(2,:);stop(2,:)];
%choose maxPlot evenly spaced
nPossible = size(x,2);
if nPossible > maxPlot
    plotIndex = round(linspace(1,nPossible,maxPlot));

```

```

else
    plotIndex = 1:nPossible;
end
plot(x(:,plotIndex),y(:,plotIndex),'r')
%plot rays inside lens
start = lensEnterPoints;
center = [zeros(1,numRays_perObjectPoint); yIntercept_PassingLensCenter];
stop = lensExitPoints;
xLEFT = [start(1,:);center(1,:)];
yLEFT = [start(2,:);center(2,:)];
plot(xLEFT(:,plotIndex),yLEFT(:,plotIndex),'r')
xRIGHT = [center(1,:);stop(1,:)];
yRIGHT = [center(2,:);stop(2,:)];
plot(xRIGHT(:,plotIndex),yRIGHT(:,plotIndex),'r')
%plot rays from lens to fpa
start = lensExitPoints;
stop = fpaPoints;
x = [start(1,:);stop(1,:)];
y = [start(2,:);stop(2,:)];
plot(x(:,plotIndex),y(:,plotIndex),'r')
% parameters of plot:
plotLimit = max(lensRadius,detectorRadius)*1.5;
xlim([-plotLimit,plotLimit])
ylim([-plotLimit,plotLimit])
set(gca,'XTick',[]);
set(gca,'YTick',[]);
title('Diagram of Optical System and Detector','FontSize',16,'FontWeight','bold')
xlabel('millimeters','FontSize',14,'FontWeight','bold')
ylabel('millimeters','FontSize',14,'FontWeight','bold')
saveas(gcf,[clipname,'z1'],'fig');
saveas(gcf,[clipname,'z1'],'jpg');
%saveas(gcf,[clipname,'z1'],'emf');
saveas(gcf,[clipname,'z1'],'eps');

% 4c) Point Spread Function:
% 4c1) Compute PSF:
%FPA histogram
%figure;
rayPoints = real(fpaPoints)-repmat(fpaCenter,1,nLensEnterPoints);
angle = asin(rayPoints(2,:)./detectorRadius);
binEdges = linspace(-pi/2,pi/2,nPSF_sampleBins);
binWidth = mean(diff(binEdges));
count = histc(angle,binEdges);
%bar(binEdges,count,'histc')
xlabel(['angle (rad), bin size = ',num2str(binWidth),' rad'])
ylabel(['count ( ',num2str(numObjectPoints),' object points, ',num2str(sum(count)),' rays )'])
%grid on
% 4c2) Plot PSF:
figure;
set(gcf,'ToolBar','figure');

```



```

set(gcf, 'OuterPosition', outerPosition__full_figure())
set(gcf, 'Position', position__full_figure())
pause on
pause(1)
binCenters = binEdges(1:end-1) + diff(binEdges)/2;
countDensity = count/binWidth;
density = countDensity/sum(count);
plot(1000*binCenters, density(1:end-1));
set(gca, 'yscale', 'log')
grid on
set(gca, 'xlim', [-pi/2, pi/2])
xlabel('Angle (mrad)', 'FontSize', 14, 'FontWeight', 'bold')
ylabel('Magnitude', 'FontSize', 14, 'FontWeight', 'bold')
title('Point Spread Function, Optical Aberrations', 'FontSize', 16, 'FontWeight', 'bold')
xMIN = 1000*binCenters(find(density>0, 1, 'first'));
xMAX = 1000*binCenters(find(density>0, 1, 'last'));
%xlim([max(-pi/2, 1.4*xMIN - 0.4*xMAX), min(pi/2, 1.4*xMAX - 0.4*xMIN)]);
% use constant scaled display, always 6.2 mm wide
xAVG = 0.5*(xMIN+xMAX);
xlim([xAVG - 3.1, xAVG + 3.1]);
yMAX = 1.5 * max(density);
ylim([yMAX/1000, yMAX])
saveas(gcf, [clipname, 'z2'], 'fig');
saveas(gcf, [clipname, 'z2'], 'jpg');
%saveas(gcf, [clipname, 'z2'], 'emf');
saveas(gcf, [clipname, 'z2'], 'eps');

% 4d) MTFs:
% 4d1) Optical Aberration MTF
%Optical Modulation Transfer Function (in cyc/rad)
fig = figure;
set(gcf, 'ToolBar', 'figure');
set(gcf, 'OuterPosition', outerPosition__full_figure())
set(gcf, 'Position', position__full_figure())
pause on
pause(1)
f = fft(density*binWidth);
M = abs(f);
CycPerRad = (0:numel(M)-1)/(pi);
plot(CycPerRad, M, '-');
xlabel('Spatial Frequency (cyc/rad)', 'FontSize', 14, 'FontWeight', 'bold')
%xlim([0, (numel(M)/2)/(pi)])
% force plot size!!:
xlim([0, 420])
hold on
ylabel('Normalized Modulation Depth', 'FontSize', 14, 'FontWeight', 'bold')
grid on

% 4d2) Detector MTF (100% fill factor)
theory = sin(CycPerRad.*pixWidth*pi)./(CycPerRad.*pixWidth*pi);
%plot(CycPerRad, abs(theory), 'k')

```

```

legend({'Optical MTF'}, 'FontSize', 14)
%text(420, 0.83, ['Detector Pixel Size = ', num2str(pixWidth*1000), ' mrad = ', ...
               %num2str(pixWidth*detectorRadius*10^6), '
\mum'], 'FontSize', 14)
% xlim([0, 100])
ylim([0, 1])

% 4d3 Draw 68 cyc/mm line for reference:
cycpmm = CycPerRad/(detectorRadius*1000);
maxFreq = 68; %cycles per mm
maxFreq_in_cycperrad = maxFreq * (detectorRadius * 1000); % converted from mm^-1 to
rad^-1;
% draw a line at maxFreq on the MTF plot:
plot([maxFreq_in_cycperrad, maxFreq_in_cycperrad], [0, 1], 'k', 'LineWidth', 1.5)
text(maxFreq_in_cycperrad+2, 0.88, '68 cyc/mm', 'Color', 'k')
text(maxFreq_in_cycperrad+2, 0.86, 'Line', 'Color', 'k')
%text(410, 0.91, '(6.0 mm)', 'Color', 'k')
title('Modulation Transfer Function, Optical Aberrations', 'FontSize',
16, 'FontWeight', 'bold')
saveas(gcf, [clipname, 'z3'], 'fig');
saveas(gcf, [clipname, 'z3'], 'jpg');
%saveas(gcf, [clipname, 'z3'], 'emf');
saveas(gcf, [clipname, 'z3'], 'eps');

% 4d4 Replot Optical MTF in cyc/mm (measured on detector)
figMM = figure;
set(gcf, 'ToolBar', 'figure');
set(gcf, 'OuterPosition', outerPosition__full_figure())
set(gcf, 'Position', position__full_figure())
pause on
pause(1)
plot(cycpmm, M, '-.')
xlabel('Spatial Frequency (cyc/mm)', 'FontSize', 14, 'FontWeight', 'bold')
%xlim([0, (numel(M)/2)/(pi)])
% force plot size!!:
hold on
ylabel('Normalized Modulation Depth', 'FontSize', 14, 'FontWeight', 'bold')
legend({'Optical MTF'}, 'FontSize', 14)
xlim([0, 68])
ylim([0, 1])
set(gca, 'XTick', 0:17:68);
grid on
title('Modulation Transfer Function, Optical Aberrations', 'FontSize',
16, 'FontWeight', 'bold')
saveas(gcf, [clipname, 'z4'], 'fig');
saveas(gcf, [clipname, 'z4'], 'jpg');
%saveas(gcf, [clipname, 'z3'], 'emf');
saveas(gcf, [clipname, 'z4'], 'eps');

```

```

%{
%Optical MTF in terms of cycles per mm (on FPA surface)
figure;
plot(cycpmm,M)
xlim([0,maxFreq])
xlabel('Spatial Frequency on Detector (cyc/mm)','FontSize',14,'FontWeight','bold')
ylim([0,1])
if maxFreq > ((numel(M)/2)/pi)/(detectorRadius*1000)
    title(['WARNING: PSF sampled at nyquist = ',num2str(((numel(M)/2)/pi)/
(detectorRadius*1000)),...
' cyc/mm, increase
nPSF_sampleBins'])
end
ylabel('Normalized Modulation Depth','FontSize',14,'FontWeight','bold')

%Confirm Optical MTF by examining normalized modulation depth of object
%test pattern convolved with angular point spread function
figure;
fpaSpace = binCenters*detectorRadius*1000; %FPA coordinates in mm
% testFrequency = 10; %cyc per rad
testFrequency = 1*(detectorRadius*1000); %cyc per rad
objSignal = (sin(binCenters*testFrequency*2*pi)+1)/2;

objModulationDepth = (max(objSignal)-min(objSignal))/(max(objSignal)+min(objSignal));
imgSignal = conv(density(1:end-1)*binWidth,objSignal,'same');

%sampleIndex = round(numel(imgSignal)/3):round(2*numel(imgSignal)/3);
sampleIndex = round(2*numel(imgSignal)/5):round(3*numel(imgSignal)/5);
    %calculate image modulation depth avoiding edge effects
sample = imgSignal(sampleIndex);
imgModulationDepth = (max(sample)-min(sample))/(max(sample)+min(sample));
plot(fpaSpace,objSignal)
hold on
plot(fpaSpace,imgSignal,'r')
plot(fpaSpace(sampleIndex),sample,'k','linewidth',3)
title(['Object Frequency = ',num2str(testFrequency/(detectorRadius*1000)),...
' cyc/mm, Object Modulation Depth = ',num2str(objModulationDepth),...
', Image Modulation Depth = ',num2str(imgModulationDepth)])
legend(['Object Signal','Image Signal','Image Signal used for calculating image
modulation depth'])
xlabel('mm off axis on FPA')

%add coordinates to MTF plot
figure(fig)
plot(testFrequency,imgModulationDepth,'k+','markersize',20,'linewidth',2)

%}

```


Illustrations

Figures

Figure 1-1. Two Usages of the Term Pixel: (a) Pixel Pattern as Used in Imaging and (b) Physical Pixels (Bottom) Forming an FPA, With Micro Lenses (Top) and Color Filters (Center)	1-1
Figure 1-2. Cutout of a Camera Showing the Lens System and the Position of the FPA	1-2
Figure 1-3. Comparison of Ray Tracings for Different Systems	1-2
Figure 4-1. The Spatial Frequency of an Object Pattern With the Resulting Image Pattern at Different Spatial Frequencies	4-2

Abbreviations

2-D	two-dimensional
3-D	three-dimensional
AMDS	Advanced Mine Detection System
DARPA	Defense Advanced Research Projects Agency
EOD	Explosive Ordnance Disposal
FOV	field-of-view
GRIN	Gradient Index of Refraction
HARDI	Hemispheric Array Detector for Imaging
IDA	Institute for Defense Analyses
LSA	longitudinal spherical aberration
MTF	modulation transfer function
MTO	Microsystems Technology Office
PSF	point spread function
UAV	unmanned aerial vehicle

REPORT DOCUMENTATION PAGE*Form Approved*
OMB No. 0704-0188

Public reporting burden for this collection of information is estimated to average 1 hour per response, including the time for reviewing instructions, searching existing data sources, gathering and maintaining the data needed, and completing and reviewing this collection of information. Send comments regarding this burden estimate or any other aspect of this collection of information, including suggestions for reducing this burden to Department of Defense, Washington Headquarters Services, Directorate for Information Operations and Reports (0704-0188), 1215 Jefferson Davis Highway, Suite 1204, Arlington, VA 22202-4302. Respondents should be aware that notwithstanding any other provision of law, no person shall be subject to any penalty for failing to comply with a collection of information if it does not display a currently valid OMB control number. **PLEASE DO NOT RETURN YOUR FORM TO THE ABOVE ADDRESS.**

1. REPORT DATE January 2011		2. REPORT TYPE Final		3. DATES COVERED (From-To) July 2010 – January 2011	
4. TITLE AND SUBTITLE Military Applications of Curved Focal Plane Arrays Developed by the HARDI Program				5a. CONTRACT NUMBER DASW01-04-C-0003	
				5b. GRANT NUMBER	
				5c. PROGRAM ELEMENT NUMBER	
6. AUTHOR(S) Bohdan Balko Isaac Chappell John Franklin Robert Kraig				5d. PROJECT NUMBER	
				5e. TASK NUMBER DA-2-3256	
				5f. WORK UNIT NUMBER	
7. PERFORMING ORGANIZATION NAME(S) AND ADDRESS(ES) Institute for Defense Analyses 4850 Mark Center Drive Alexandria, VA 22311-1882				8. PERFORMING ORGANIZATION REPORT NUMBER IDA Document NS D-4268 Log: H11-000208	
9. SPONSORING/MONITORING AGENCY NAME(S) AND ADDRESS(ES) Defense Advanced Research Projects Agency Defense Sciences Office 3701 N. Fairfax Drive Arlington, VA 22203-1714				10. SPONSOR/MONITOR'S ACRONYM(S)	
				11. SPONSOR/MONITOR'S REPORT NUMBER(S)	
12. DISTRIBUTION/AVAILABILITY STATEMENT Approved for public release; distribution is unlimited. (6 May 2011)					
13. SUPPLEMENTARY NOTES					
14. ABSTRACT Curved focal plane arrays (FPAs) coupled with ball lenses can reduce spherical aberration, increase the field of view (FOV), and reduce the weight and cost of optical systems. These improvements over flat FPAs promise major upgrades for military systems. The Institute for Defense Analyses (IDA) has been investigating the potential applications of curved FPAs that are being developed in the Defense Advanced Research Projects Agency (DARPA) Hemispherical Array Detector for Imaging (HARDI) program. Several applications have been identified, but the initial focus has involved cameras mounted on small robots used for mine detection and neutralization. These cameras can be improved by the application of curved FPAs. IDA developed a ray tracing code to analyze improvement in camera resolution and conducted tradeoff studies to obtain optimum conditions for various robot camera applications.					
15. SUBJECT TERMS curved focal plane array (FPA), Defense Advanced Research Projects Agency (DARPA), Hemispherical Array Detector for Imaging (HARDI), robots, wide field of view (FOV) cameras					
16. SECURITY CLASSIFICATION OF:			17. LIMITATION OF ABSTRACT SAR	18. NUMBER OF PAGES 88	19a. NAME OF RESPONSIBLE PERSON Dr. Devanand Shenoy
a. REPORT Uncl.	b. ABSTRACT Uncl.	c. THIS PAGE Uncl.			19b. TELEPHONE NUMBER (include area code) 571-218-4932

